Surveys in Geophysics (2023) 44:463–494
https://doi.org/10.1007/s10712-022-09746-9

Toward the Scientific Interpretation of Geophysical Well Logs: Typical Misunderstandings and Countermeasures

Jin Lai[1,2] · Guiwen Wang[1,2] · Qixuan Fan[2] · Fei Zhao[2] · Xin Zhao[2] · Yuhang Li[2] · Yidi Zhao[2] · Xiaojiao Pang[2]

Received: 25 April 2022 / Accepted: 11 October 2022 / Published online: 8 November 2022

Abstract

Geophysical well log data are widely used in the field of structural geology, sedimentary geology and petroleum geology. Gaps and misunderstandings are still existing in the scientific interpretation of geophysical well logs. Logging environments and log curves need correction and standardization before interpretation, additionally, there are some special geological phenomena that will mislead the well log interpretation. This review critically highlights the typical misunderstandings existing in the well log data interpretation, and proposes countermeasures as well as scientific interpretation of well logs when encounter these misunderstandings. The factors that affect the well log data acquisition are summarized in terms of types of drilling muds, borehole stability and logging instrument rotation. The vertical resolution of various log series spans a wide range from 5 mm to about 10 m. In the field of structural geology, well logs can be used for determination of stratum attitude, fault recognition, fracture and in situ stress characterization as well as unconformity identification. Lithology and depositional facies can be interpreted using well logs. Well logs aim at finding hydrocarbons, and are used for source rock characterization and logging reservoir evaluation in the petroleum geology field. Then the typical misunderstandings and countermeasures in solving geological issues using geophysical well logs are reviewed from published papers as well as from the authors' personal experiences. This review will provide insights into the scientific interpretation of geophysical well log data, and help solving geological issues for the petrophysicist and geologist.

Keywords Geophysical well log · Misunderstandings and countermeasures · Well log interpretation · Structural geology · Sedimentary geology · Petroleum geology

✉ Jin Lai
sisylaijin@163.com

✉ Guiwen Wang
wanggw@cup.edu.cn

[1] State Key Laboratory of Petroleum Resources and Prospecting, China University of Petroleum (Beijing), 18 Fuxue Road, Changping, Beijing 102249, China

[2] College of Geosciences, China University of Petroleum (Beijing), Beijing 102249, China

Article Highlights

- Geophysical logs are used in the fields of structural geology, sedimentary geology and petroleum geology
- Typical misunderstandings in solving geological issues using well logs are reviewed
- Countermeasures are proposed for a more scientific interpretation of well logs

1 Introduction

Geophysical well logs, which record the acoustic, electrical, nuclear physical properties of the borehole walls, are widely used in solving issues in the field of structural geology, sedimentary geology and petroleum geology (Rybacki et al. 2016; Masoudi et al. 2017; Iqbal et al. 2018; Lai et al. 2018; Shan et al. 2021; Okoli et al. 2021). The continuous and high resolution well log data can overcome the limitation of high cost but low recovery core data, and therefore are of utmost importance for geologists, petrophysicists and reservoir engineers (Ellis and Singer 2007; Khoshbakht et al. 2012; Aghli et al. 2016; Lai et al. 2017; Masoudi et al. 2017; Qadri et al. 2019; Al-Mudhafar 2020). However, well log interpretation is equivocal, and there are some factors affecting the well log data acquisition. In addition, there are incompatibilities existing between geological interpretation and well log data, and some special geological phenomenon will mislead the well log interpretation process.

Nowadays, significant research efforts have been focused on the application of well logs in geological fields (Passey et al. 1990; Ameen et al. 2012; Brekke et al. 2017; Iqbal et al. 2018; Lai et al. 2018; Shalaby et al. 2019; Zhao et al. 2020; Nian et al. 2021; Haque et al. 2022). However, there are no systematic studies performed on reviewing the typical misunderstandings in the well log interpretation. Additionally, there are no related countermeasures proposed when encountering these misunderstandings during well log interpretation. Consequently, insights should be provided into the typical misunderstandings in well log interpretation, and countermeasures are needed to be proposed for a more scientific interpretation of geophysical well logs (Lai et al. 2022a).

This review starts with clarifying the factors which will affect the well log data acquisition, and points out that types of drilling muds, borehole wall stability as well as instrument will mislead the well log interpretation process. Then the wide range of vertical resolution from 5 mm to 10 m of various well log suits are summarized. In the structural geology field, well log data are used for stratum attitude (dip direction and dip angle) determination, recognition of fault, fracture characterization, and in situ stress analysis, and unconformity evaluation. Then the typical misunderstandings that will influence the application of well logs in structural geology fields are summarized. In the field of sedimentary geology, well logs are used for lithology recognition, and depositional facies interpretation. Then the special lithology (high gamma sandstone) and cemented minerals (carbonate) that will mislead the well log interpretation are clarified. In the field of petroleum geology, well logs mainly aim at source rock characterization and logging reservoir evaluation. Then advanced well log series are integrated to evaluate the low resistivity oil layers as well as unconventional oil and gas resources. This review is hoped to fill the gap existing in solving geological issues using well logs, and have theoretical guidance and technical support for beginners and interested readers.

2 Well Log Data Acquisition

The acquisition of geophysical well logs are largely dependent on the logging environments (including types of drilling muds and borehole wall stability) and stability of log instruments. Therefore in order to avoid mistaken interpretation, the quality of well log data, which will be influenced by drilling mud types, borehole wall stability and instrument rotation, should be evaluated and corrected before interpretation.

2.1 Types of Drilling Muds

The drilling muds can be divided into oil based and water based (Lai et al. 2017; Qadri et al. 2022), and the water based drilling muds can be further divided into fresh water and salty water. In water based drilling muds, the deep resistivity logs (resistivity curves with deep depth of investigation) are generally larger than the shallow resistivity logs, and the positive separation (M2Rx > M2R1) will be encountered (Fig. 1A). The M2R1-M2Rx well log suits are high-definition resistivity logs, and M2R1 has a depth of investigation of 10 in (25.4 cm), while the depth of investigation of M2Rx is 120 in (3.048 m), and M2R2, M2R3, M2R6, M2R9 correspond to 20 in, 30 in, 60 in and 90 in depths of investigation. Conversely, in oil based drilling muds, the shallow resistivity logs are commonly greater than deep resistivity logs, indicating a negative separation (M2Rx < M2R1) (Fig. 1B).

The resistivity logs have no ability to differentiate the fresh and salty water based drilling muds, and therefore the spontaneous potential (SP) log and natural gamma ray (GR) log should be integrated. In fresh water based drilling mud, the SP log has the same trend with GR log. In other words, the SP log for sandstone intervals, which are characterized by log GR values, have negative trends (Fig. 2A). Conversely, for the salty water based drilling muds, the SP log has an opposite trend with GR log (Fig. 2B). As can be seen in Fig. 2B, the low GR sandstone intervals correspond to the high SP readings (Fig. 2B).

2.2 Borehole Wall Stability

There are many well log suits pasted around the borehole during logging, and they include the bulk density (DEN), micro resistivity logs (Micro Spherically Focused Log: MSFL), nuclear magnetic resonance (NMR), and electrical image log, etc. Consequently, the borehole regularity will affect the behaviors of the above well log series. In Fig. 3, the borehole wall in the interval 3400–3450 m encounters collapse, and the borehole collapse is recognized by the evident increasing CAL log. As a result, the DEN log is significantly reduced and the AC is increased (Fig. 3). The micro resistivity log (RI) is reduced evidently due to the borehole collapse, while the Rxo and Rt are also decreased (Fig. 3). Furthermore, the NMR log, which provide the T_2 (transversal relaxation time) spectrum, has an abnormal behavior in the collapse interval. The amplitude of T_2 spectrum becomes much higher, and in some cases contain tail distribution, which are not the reflection of formation but instead the drilling muds (Fig. 3). The borehole collapse will result in the abnormal low bulk density, low resistivity, high sonic transit time and high amplitude of T_2 spectrum (Fig. 3).

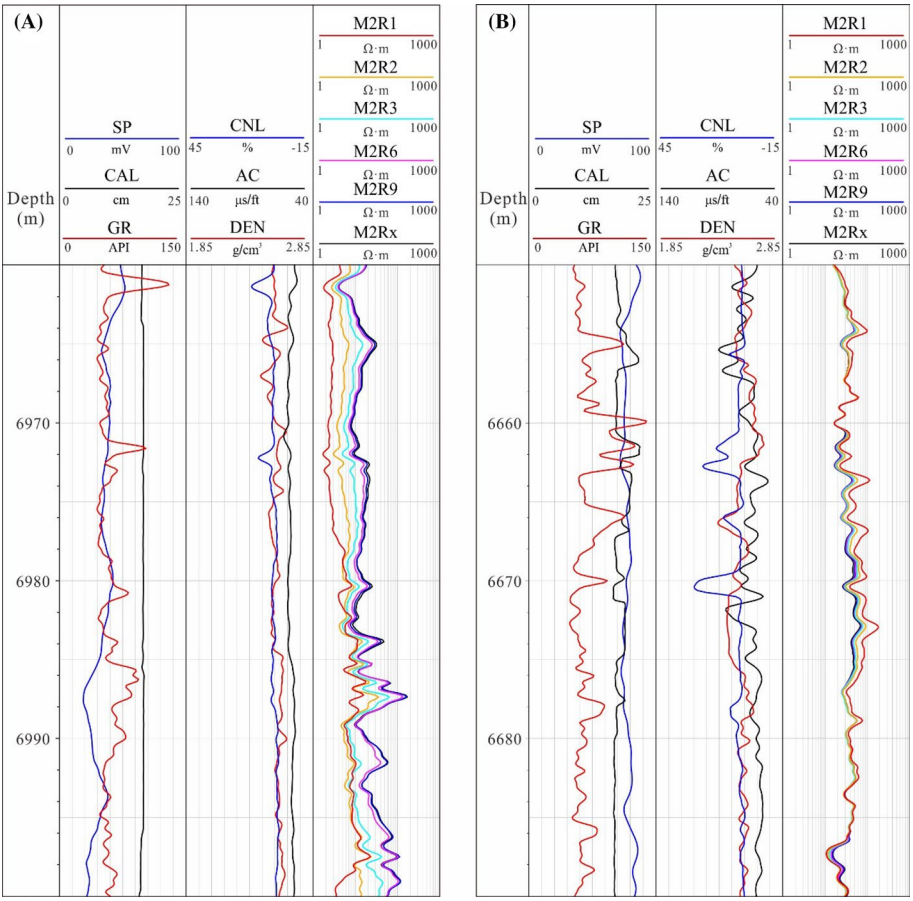

Fig. 1 Water and oil based drilling muds expressed from conventional log suits. **A** Water based drilling muds with deep resistivity logs are higher than shallow logs, Well KS 207; **B** Oil based drilling muds, Well KS 206

2.3 Instrument Rotation

There are some logging tools which will be kept rotating during logging, and they include the dipmeter log, array sonic log and electrical image log. The azimuth curve (AZOD) will record the rotation process during logging (Fig. 4). The sonic image logging tool (UBI: ultrasonic borehole image) is also keeping rotated during logging. The normal rotation of UBI logging tool has no effect of the data quality (6775–6780 m) (Fig. 4), however, the abnormal rotation of UBI logging tool will result in the poor quality and even mistaken appearances of ultrasonic borehole image patterns (6763–6773 m) (Fig. 4).

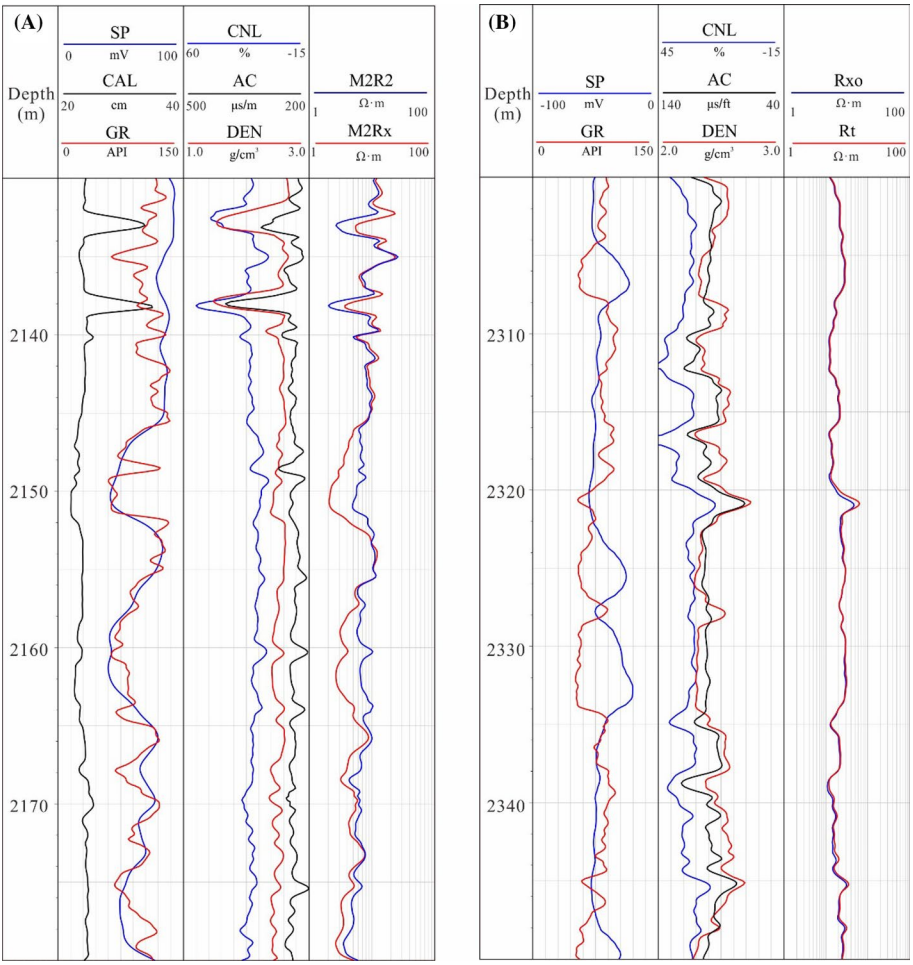

Fig. 2 Types of drilling muds (fresh and salty water) expressed from conventional log suits. **A** Fresh water drilling muds, SP curve is consistent with GR log, Well Huang 115. **B** Salty water drilling mud, SP curve has a reverse trend with GR log, Well NP 2-1

3 Vertical Resolution of Various Well Log Data

Vertical resolution of various log suites ranges from millimeter (electrical image logs), centimeters (Micro Spherically Focused Log, MSFL), to about 1 m (natural Gamma Ray, GR) (Masoudi et al. 2017) (Fig. 5). Core observation and core analysis data can provide insights into the geological features up to nanometer scales. However, none of the well log series can capture the nanometer scale variation of formation. Electrical image logs, which measure the electrical resistivity of borehole wall, provide the highest vertical resolution of 5 mm (Folkestad et al. 2012; Lai et al. 2018). The dissolution vugs on the core observation are captured by the image logs as dark spots (Fig. 5) (Masoudi et al. 2017; Lai et al. 2020).

Conventional well log series, which include spontaneous potential (SP), natural gamma ray (GR), sonic interval transit time (AC), compensated neutron log (CNL), bulk

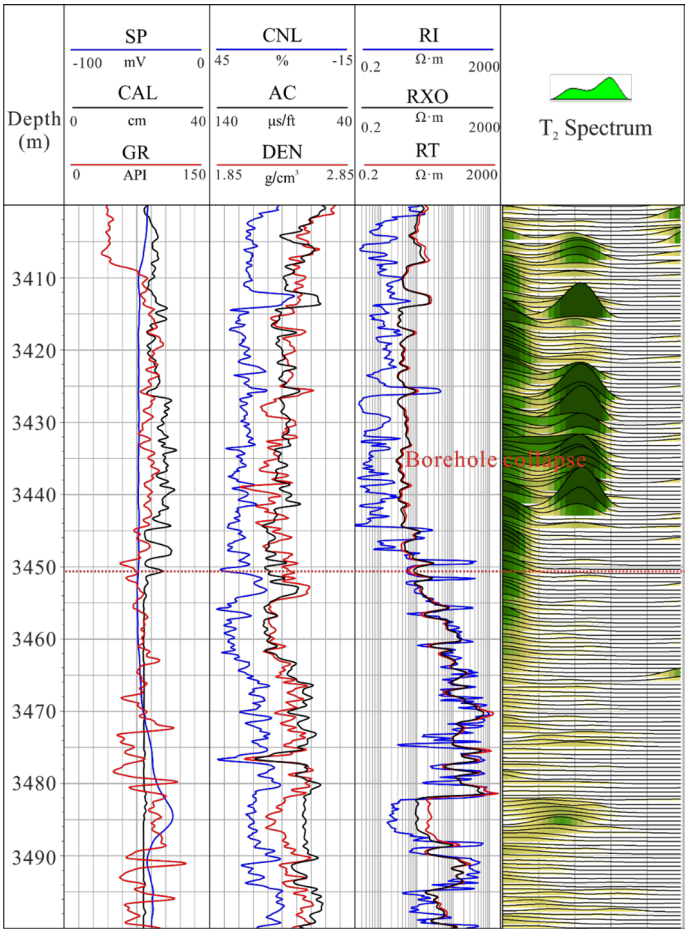

Fig. 3 Borehole collapse and related conventional as well as NMR log expressions (Well Ji 10024)

density (DEN) and three resistivity logs with various depth of investigation, are characterized by vertical resolutions of about 1 m (Fig. 5). The beds thinner than 0.6096 m (2 ft) cannot be properly evaluated by conventional well logs (Fig. 5). Therefore, thin layer of coals or mudstones cannot be characterized by conventional logs since they are below the resolution of conventional logs. However, the high-definition induction logs (HDIL) can provide a vertical resolution of 1–2 ft (Fig. 5).

Sonic and neutron porosity logs, which measure the sonic transit time and hydrogen content of a formation, are useful for lithology identification and porosity estimation (Zazoun 2013; Aghli et al. 2016). Density log measures the bulk density of formation according to the Compton effect, and is commonly used for porosity calculation and recognition of gas layers. In addition, the litho-density (Pe) log can also be used to recognize lithology and even estimate brittleness index (Lai et al. 2015). Therefore in the vuggy or fractured zone, the sonic transit time and neutron porosity logs will be

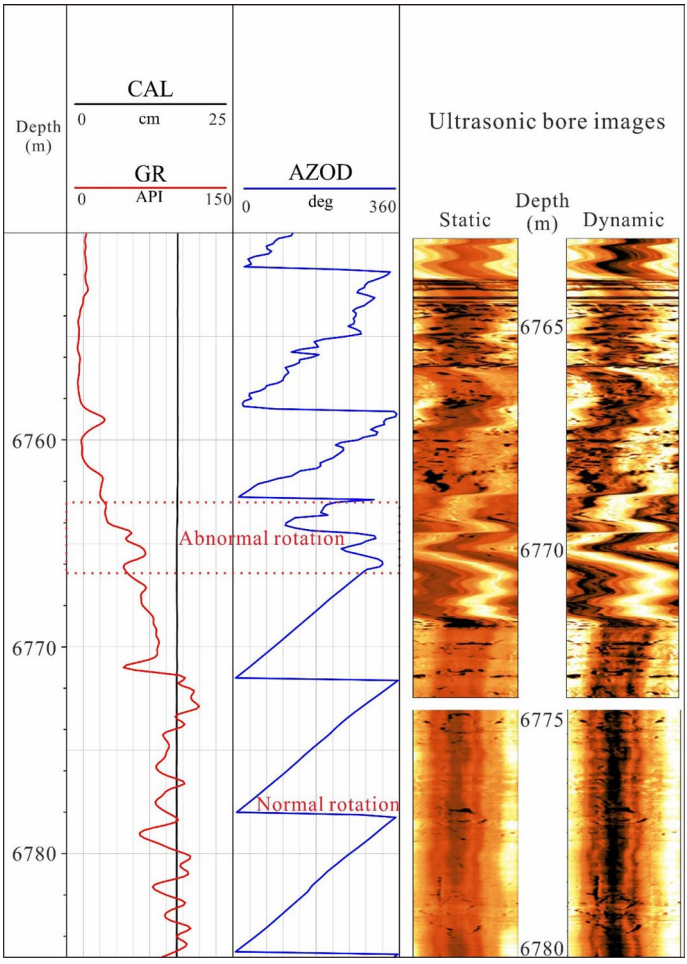

Fig. 4 Image pattern due to abnormal rotation of ultrasonic borehole imaging (UBI) logging tool (Well KS 8004)

increased due to the enlarged pore spaces, however, the bulk density will be decreased (Aghli et al. 2016; Moussavi-Harami and Mohammadian 2016; Lai et al. 2017).

Array acoustic logs have a vertical resolution of 3.0 m, and can characterize the in situ stress fields and fracture (Collett et al. 2011; Zaree et al. 2016). Sonic logs are the most applicable logs in seismic petrophysics and rock physics. Therefore the sonic logs (both compressional and shear logs) should be evaluated carefully in heterogeneous reservoirs. Sonic *V*p/*V*s is a function of lithology, porosity type, and they are widely used for lithology and fluid recognition, and even reservoir prediction (Russell et al. 2003; Wang et al. 2020).

The elemental capture spectroscopy (ECS) log and Nuclear Magnetic Resonance (NMR) log provide the mineral assemblage and fluid property variations of the formation with vertical resolution of 0.457 m and 0.2 m, respectively. The acoustic reflection imaging technology have the highest depth of investigation (tens of meters), and it can capture the

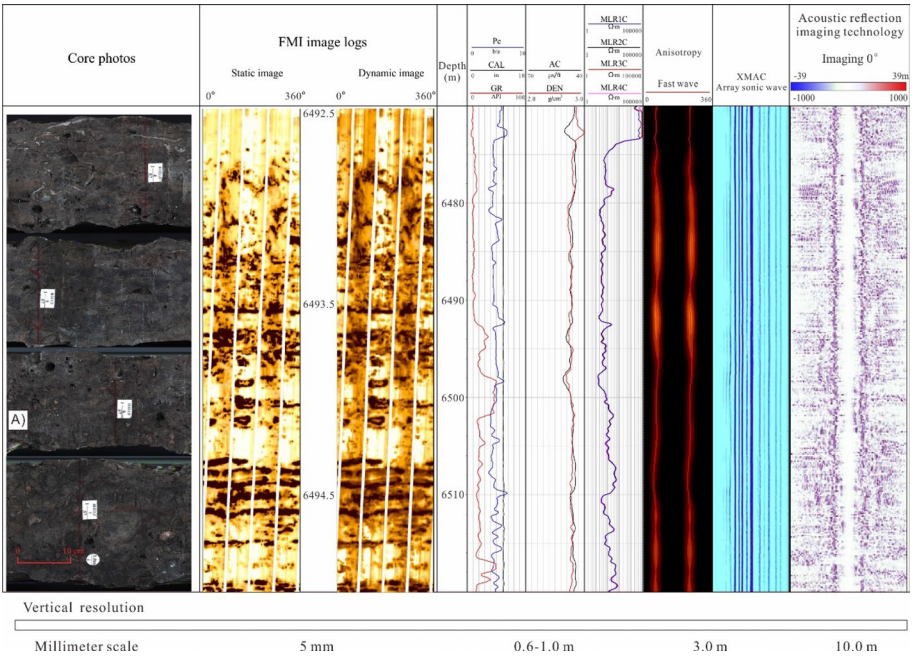

Fig. 5 Variation of vertical resolution for various geophysical well log data (Well HT 2)

cavity and fracture far away from the borehole; however, the vertical resolution is reduced to 10.0 m (Fig. 5).

Outcrop, core and related laboratory analysis data have a wide resolution range from nanometer to meter scale. Outcrop observation can describe the variation of lithology assemblage in meter-scales. Core observation will provide millimeter scale changes of lithology and sedimentary structure. Thin section optical observation will provide about 10 μm resolution of mineralogy and pore spaces. Scanning Electron Microscope (SEM) has a very high resolution up to nanometer scales. Also the nano-CT analysis will provide a nanometer scale resolution of pore throat structure. Geological analysis data have a much higher resolution than conventional well logs, therefore gaps will be existed when calibrating core data with well log data.

Due to the mismatching resolution of geological data and geophysical well logs, the rapid changes in geological properties of rocks will cause variations in petrophysical responses. As is well known, the heterogeneous carbonate rocks commonly have complex petrophysical behaviors (Lai et al. 2020). Especially the carbonate rocks are well known to be deposited in various environments, and late-stage diagenetic and fluid transformations will result in the significant heterogeneity at numerous scales (Mollajan and Memarian 2016; Tian et al. 2019; Ngia et al. 2019; Lai et al. 2021). In addition, the effect of sedimentary structures and diagenetic imprints (beddings, stylolite as well as fractures) on the well log responses cannot be ignored. The presences of beddings, stylolite and fractures will on the one hand cause the heterogeneity in rocks, on the other hand will affect logs trend. For instance, the dissolution vugs are recognized as dark spots on the image logs, and they will cause reduction in bulk density (Fig. 3).

The presences of horizontal fractures will result in the increase in sonic transit time but reduction in resistivity logs (Fig. 3).

4 Structural Geology

4.1 Attitude of Stratum

The formation in complex geological settings is characterized by high and steep structure, consequently well logs are difficult to obtain the attitude (dip and dip angles) of stratum in complex geological settings. Therefore, seismic interpretation should be integrated to calibrate with well logs to obtain the dip direction and dip angle of formation (Fig. 6). The *S–N* seismic interpretation profile reveals the complex structure in Fig. 6, and a reverse fault is encountered above the *T*6 seismic line. An anticline is interpreted between T6 and T8 line, and another reverse fault is recognized below *T*6 seismic line (Fig. 6). The formation is steep, and the dip angles can reach more than 30° (Fig. 6). The pole chart picked out from image logs confirms the steep dip angles in well DQ 5, and the dip direction changes when encounters the fault plane (Fig. 6).

4.2 Fault

Image logs can detect small-scale fault with centimeter-scale fault distance (Fig. 7). The centimeter-scale fault displacement around the borehole can be recognized by the

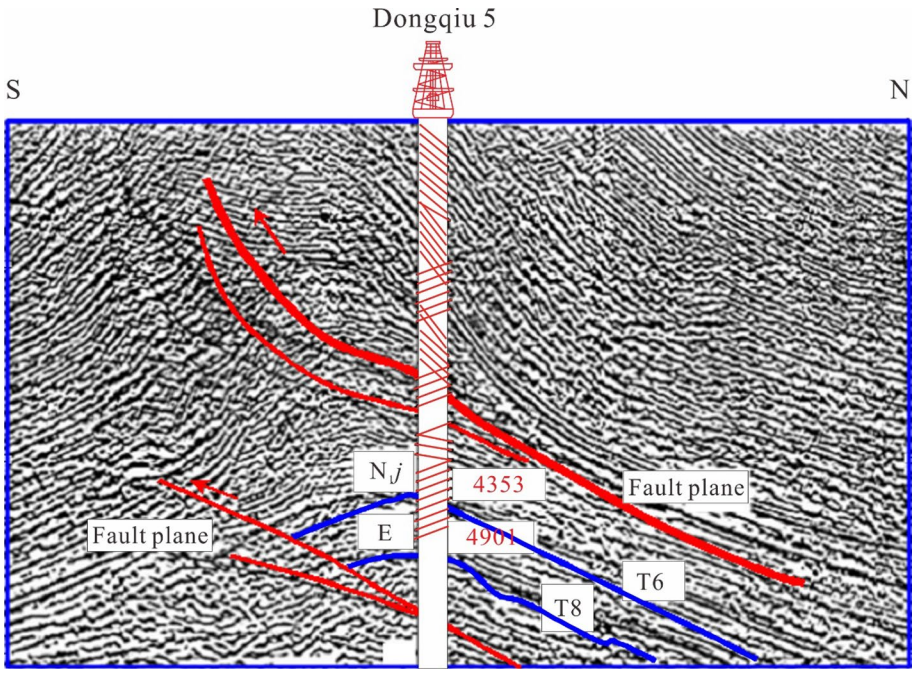

Fig. 6 Calibration of seismic line with well log to obtain the attitude of strata

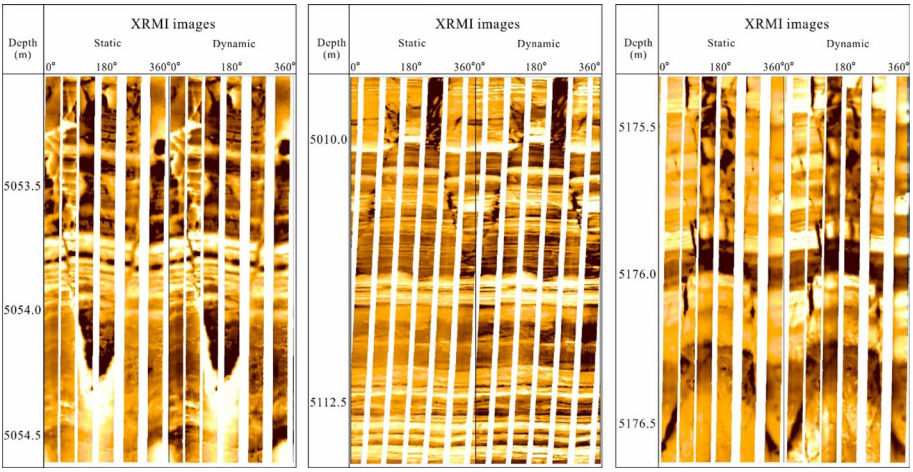

Fig. 7 Fault picked out from image logs (Well DN 205H)

discontinuous marker beds (Fig. 7). However, the image quality will be low in case of oil based drilling muds, and the presences of high resistivity gypsum will further reduce the image quality (Lai et al. 2017) (Fig. 8). Consequently, image logs may hardly capture the fault plane, therefore the pole chart and rose diagrams should be incorporated (Fig. 8). Dips are manually picked out from the images, and the dip direction is rapidly changed at the depth intervals of 6285–6295 m (Fig. 8). In addition, the rose diagram as well as the pole chart show that the dip direction is significantly varied, implying the presences of fault (Fig. 8). The cross section (interpreted from seismic profile) confirms that there is a reverse fault cutting through the intervals of 6285–6295 m (Fig. 8). The abrupt changes in image log patterns and dip patterns are commonly associated with the fault planes (Fig. 8).

4.3 Fracture and In Situ Stress

Natural fractures are one of the most important factors to enhance permeability and hydrocarbon productivity in heterogeneous reservoirs where matrix porosity is low (Aghli et al. 2019; Momeni et al. 2019; Pan et al. 2022). Natural fractures will result in the enlargement of CAL, minor decrease in DEN log, significant increase in sonic interval transit time (AC) but rapid decrease in resistivity (Jafari et al. 2012; Khoshbakht et al. 2012; Zazoun 2013; Aghli et al. 2016; Lyu et al. 2016; Ameen 2016; Nian et al. 2021; Lai et al. 2022b). However, only one type of well log cannot detect the fracture zones, therefore a combination of conventional logs is needed for fracture identification (Lai et al. 2017; Aghli et al. 2019). Sonic and bulk density logs are sensitive for the presences of fractures, while resistivity logs are good indicators for fractured intervals. In addition, large vertical and horizontal (open) fractures will result in a cycle skipping on the compressional curves since they strongly depend on the first energy arrival detection (Lai et al. 2017; Aghli et al. 2019). Conventional log series are useful tools for fracture detection due to their low cost and availability, especially when image logs and core are not available (Lai et al. 2018; Aghli et al. 2019; Momeni et al. 2019).

Fractures are recognized as continuous sinusoids on the image logs due to drilling mud invasion into fractures (Khair et al. 2015; Lai et al. 2018; Aghli et al. 2020). The

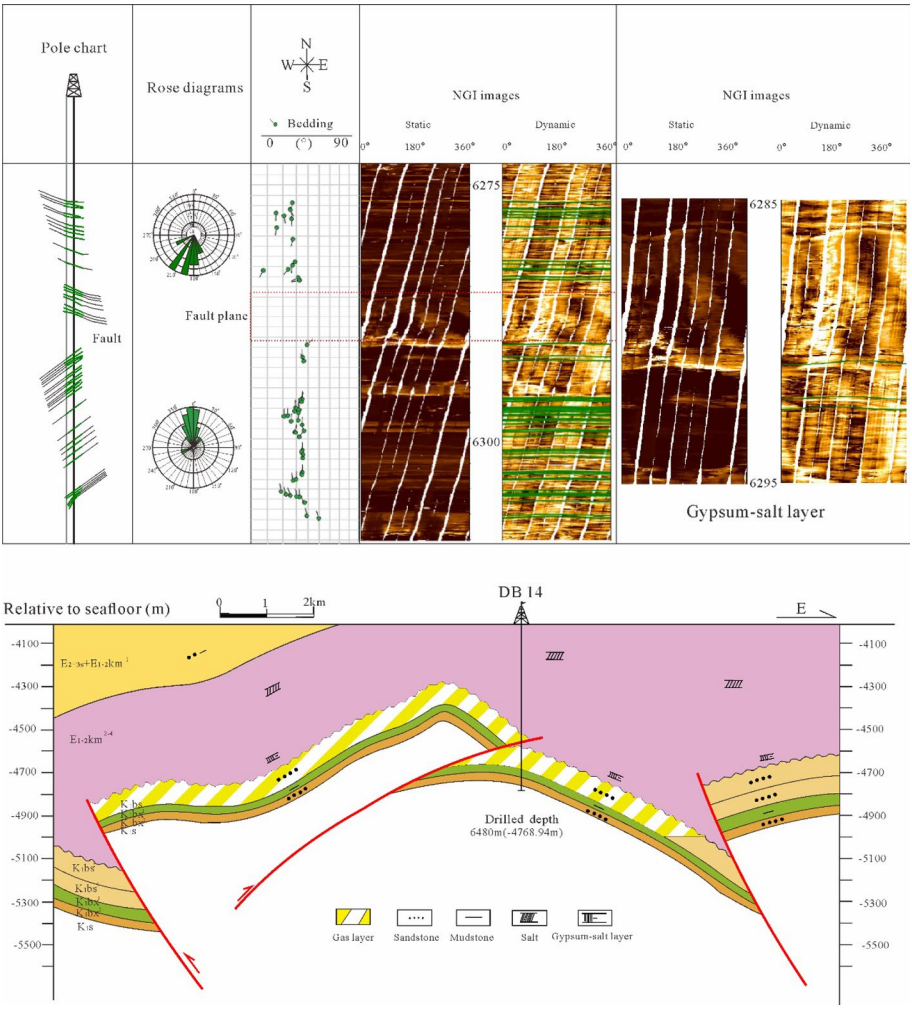

Fig. 8 Fault interpreted from the dip patterns and image logs

misunderstandings in fracture detection are that there are some geological features (beddings, mudstone layer) are difficult to be differentiated from natural fractures. For instance, faults have the same responses with fractures on conventional well logs, and only image logs can differentiate fault from fracture.

The bedding planes in sandstones have similar log responses with natural fractures (Josh et al. 2012); however, they can be differentiated from natural fractures by image logs and core observation (KS 208) (Fig. 9). In addition, the thin layered mudrocks may also have low resistivity but high sonic transit time (Fig. 9). The reduction in resistivity is due to increasing shale content, and the presences of mudstone intraclasts can be evidenced from the core and image logs. The mudstone intraclasts appearing along the bedding planes will result in the increase in sonic transit time and reduction in resistivity (Fig. 9).

Fractures in conglomerates will not cause a significant decrease in resistivity since the inherent high resistivity of conglomerates. As is seen in Fig. 10, there are two fractures

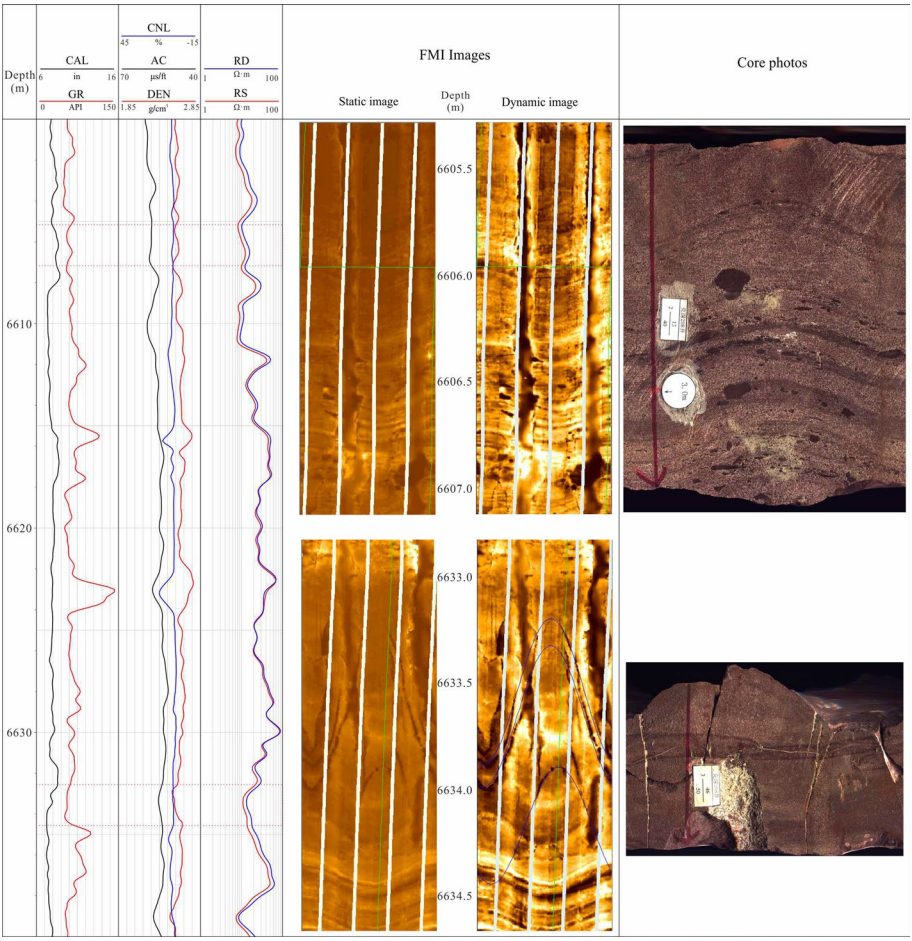

Fig. 9 Fracture prediction using conventional log, image log calibrated with core (Well KS 208). The bedding planes have similar log responses with natural fractures; however, they can be differentiated from natural fractures by image logs and core observation

recognized in the conglomerates, and the related resistivity values (LLD, LLS) are reduced to some extent (Fig. 10). In addition, the RMSL log has a rapid decrease (Fig. 10). However, the resistivity values are still much higher than the underlying siltstones (Fig. 10). The resistivity values of conglomerates even with fractures are higher than the siltstones without fractures (Fig. 10). In addition, the natural fractures in Fig. 10 only crosscut around the borehole with low extension length, and they do not extend into the surrounding rocks. They can only be detected by MSFL which have low depth of investigation of about 5–8 cm, and the high-definition induction logs as well as dual lateral resistivity logs (LLD, LLS) have no responses with theses fractures (Fig. 10).

The fractures are commonly evaluated by their porosity, aperture, length and density, which can be calculated by borehole image logs (Ameen 2014; Lai et al. 2018). Fracture porosity and fracture aperture are very essential for permeability contribution, and dual lateral logs can be used for qualitative estimation of fracture aperture and porosity (Aghli

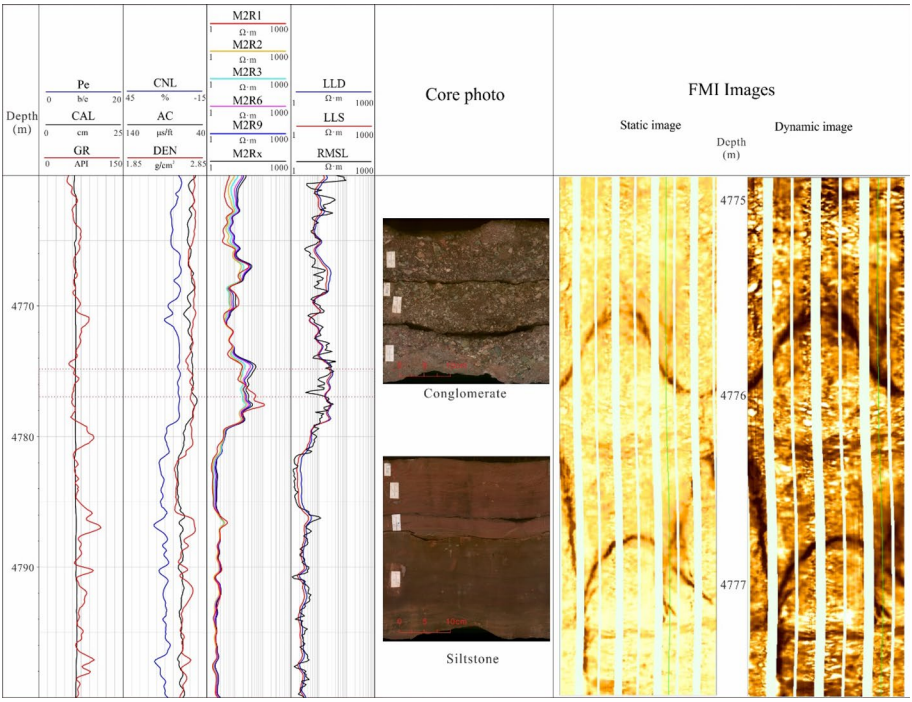

Fig. 10 Natural fractures in conglomerates with low extension lengths (Well DN 201)

et al. 2019). Misunderstandings exist in the order of magnitude of fracture parameter especially the fracture porosity. Most of fractures show microns width (Aghli et al. 2019). Though the presences of fracture may enhance permeability, the fracture porosity is commonly less than 0.5%, and can hardly reach 1% (Zeng and Li 2009). A fracture with 1 mm aperture (a very large open fracture) and 1 m length only results in a 0.1% fracture porosity (Aghli et al. 2019).

Natural fractures are considered as the fractures in a formation prior to drilling (Nelson 2001). Besides natural fracture, there are stress-induced fractures and borehole breakouts (Prioul et al. 2007; Lai et al. 2018). Drilling induced fractures (two vertical fractures with 180° apart from each other) and borehole breakouts (wellbore enlargements appearing as broad dark bands) indicate the in situ stress field (Ameen et al. 2012; Lai et al. 2018). Natural fractures can be distinguished from drilling induced fractures by their continuous nature on image logs. In addition, natural fractures often occur as continuous sinusoids (dark or bright), whereas drilling induced fractures, which are 180° apart with each other, only propagate in the tensile region of the borehole walls (Khair et al. 2015; Lai et al. 2018). Image logs can easily differentiate the drilling induced fractures and borehole breakouts, and therefore can provide the SHmax (maximum horizontal in situ stress) and Shmin (minimum horizontal in situ stress) direction (Khair et al. 2015; Lai et al. 2018; Iqbal et al. 2018). Induced fractures generally have very low extension length into the borehole, and they will result in the rapid decrease in MSFL logs, while dual lateral logs (LLS, LLD) will not be reduced (Fig. 11).

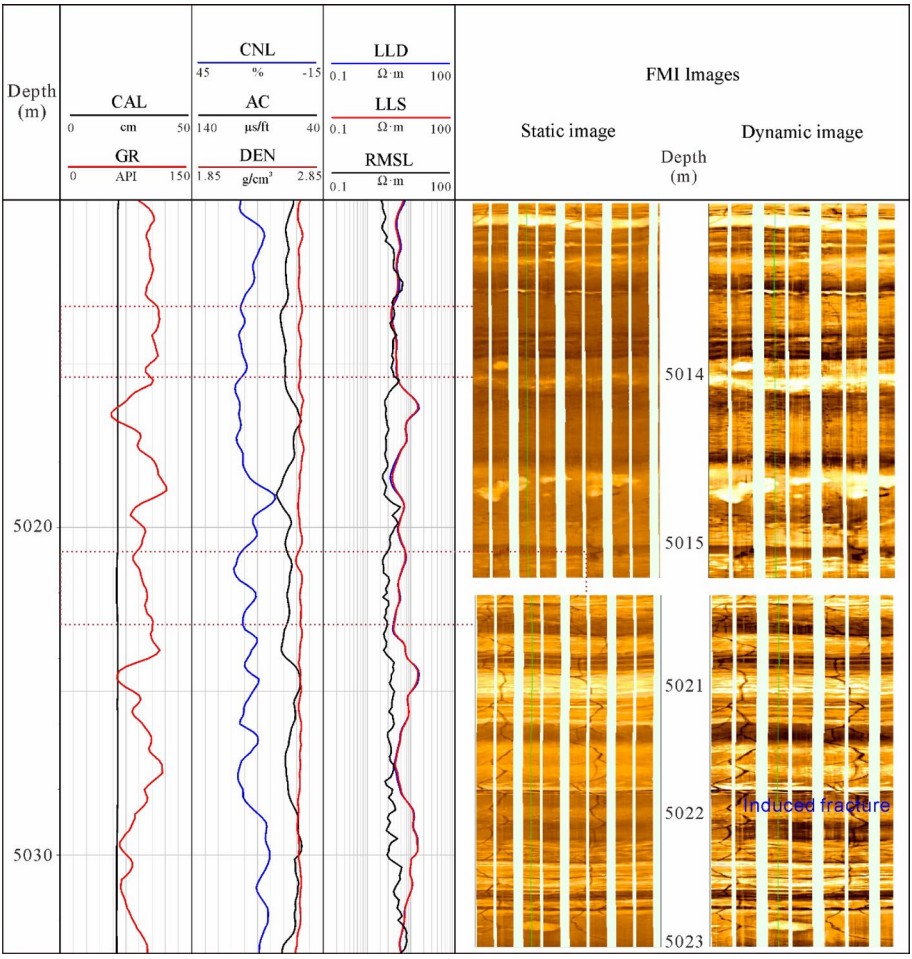

Fig. 11 Rapid decrease in MSFL log encountering induced fracture (Well DN 201). Note that the dual lateral logs will not be reduced

4.4 Unconformity

The unconformity (parallel and angular) surfaces imply a depositional hiatus and erosion of formation, and therefore have evident changes in conventional well log shapes and image log patterns (Fig. 12). The Well Shan 367 in Ordos Basin has encountered an unconformity surface between Carboniferous Benxi Formation (sandstone formed in fluvial-deltaic environments) and Ordovician Majiagou Formation (carbonate rocks formed in marine platform environments) (Wang and Al-Aasm 2002; Yang et al. 2005; Liu et al. 2009; Wang et al. 2020). The regional uplift during the late Ordovician and early Carboniferous in the Ordos basin resulted in serious erosion, and the Silurian, Devonian and Early Carboniferous strata are absent (Liu et al. 2009; Li and Li 2011).

The unconformity surface in Well Shan 367 is recognized as a rapid decrease in GR reading, but sharp increase in the resistivity logs (Fig. 12). Additionally, the three

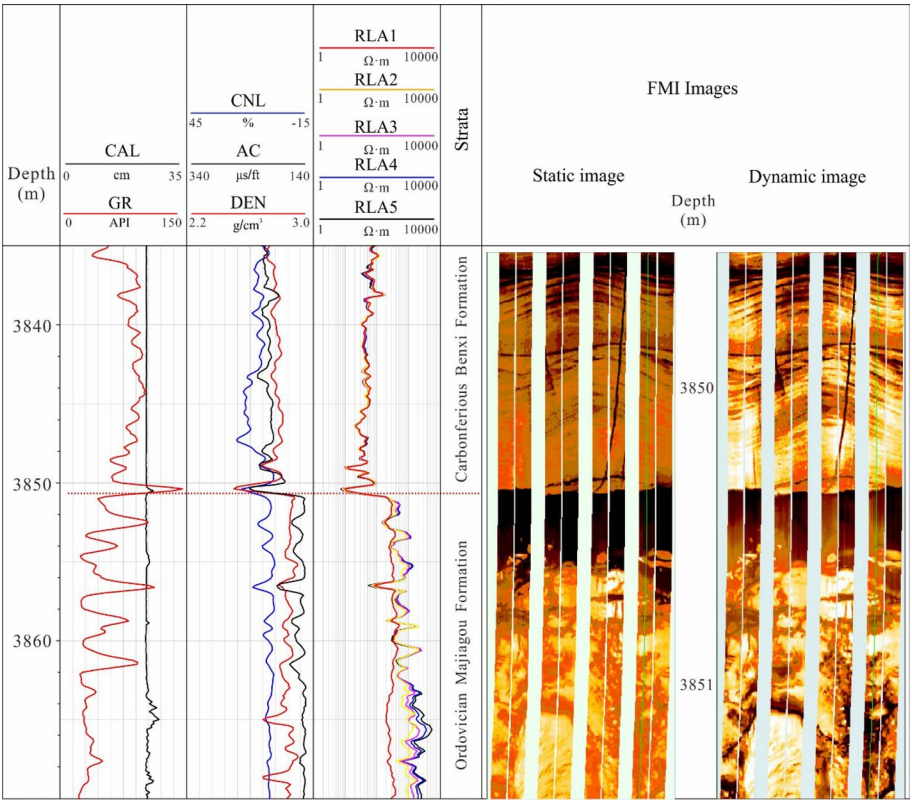

Fig. 12 Rapid change of conventional log curve morphology and image log pattern of unconformity (Well Shan 367)

porosity logs all have evident response variations between the unconformity surfaces (Fig. 12). The image log patterns change from bright bands in Bnexi Formation (sandstone) into bright spots in Majiagou Formation (dolostone), and the unconformity surface is recognized as a dark band (Fig. 12).

5 Sedimentary Geology

Understanding of lithology associations and reservoir architectures is commonly hindered due to the limited core data (Xu et al. 2009). Well logs can continuously characterize the small-scale sedimentary structures and therefore are important for facies interpretation (Donselaar and Schmidt 2005).

5.1 Special Lithology and Minerals

Conventional well logs including gamma ray (GR), bulk density (DEN), resistivity (Rt), and photoelectric factor (Pe) can reflect the variation of composition and texture (Lai et al. 2016; He et al. 2019). High resolution image logs measure grain size, rock composition,

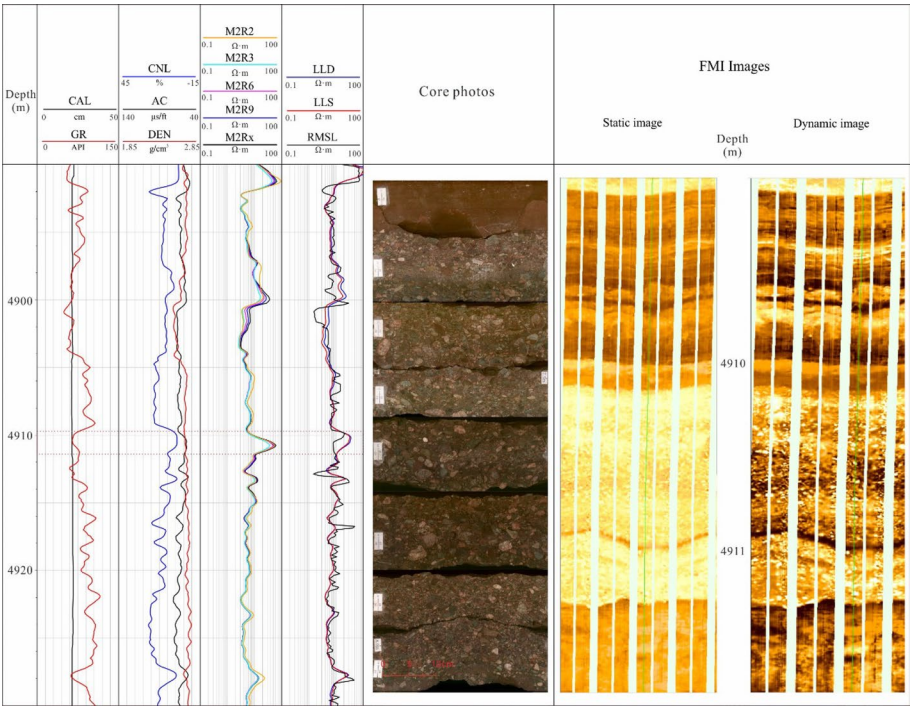

Fig. 13 Conglomerates showing low GR but high resistivity and are recognized as bright spots on image logs (Well DN 201)

bedding dips, and sedimentary structure of sedimentary rocks at the millimeter scale (Keeton et al. 2015; Brekke et al. 2017; Lai et al. 2018).

The typical misunderstandings in lithology recognition are the occurrences of special lithologies including conglomerates (Fig. 13) and mudstone pebbles (Fig. 14). Conglomerates are recognized by low GR, high resistivity, and bright spots will be appeared on the image logs (Fig. 13). However, if the pebbles are composed of mudstones, then dark spots will be identified on the image logs, and the mudstone pebbles will show low GR reading and low resistivity values (Fig. 14).

Clean sandstone will exhibit low gamma-ray values (about 15 API) (Sarhan 2019). High gamma sandstones will be encountered if there are U-rich deposits accompanied (Qiu et al. 2022). In some cases, if the sandstones are abundant in volcanic rock fragments (especially K-rick rock fragments), the logged GR readings will be high, reaching about 100 API (Fig. 15). The siltstones in Fig. 20 have GR reading about 100 API, and both the core and image logs show bedding planes (Fig. 15).

Mudstones mainly show high GR readings, but low bulk density and resistivity values (Hsieh et al. 2005; Wang et al. 2019). Both the mudrock skeletons and pore water are conductive, resulting in a low resistivity (Wang et al. 2019). However, in ultra-deeply burial settings (> 6000 m), mudstones will be tightly compacted due to the high overburden rocks, and the bulk density will be higher than the surrounding sandstones (Fig. 16). The bulk density of mudstones reaches as high as 2.7 g/cm^3, which is

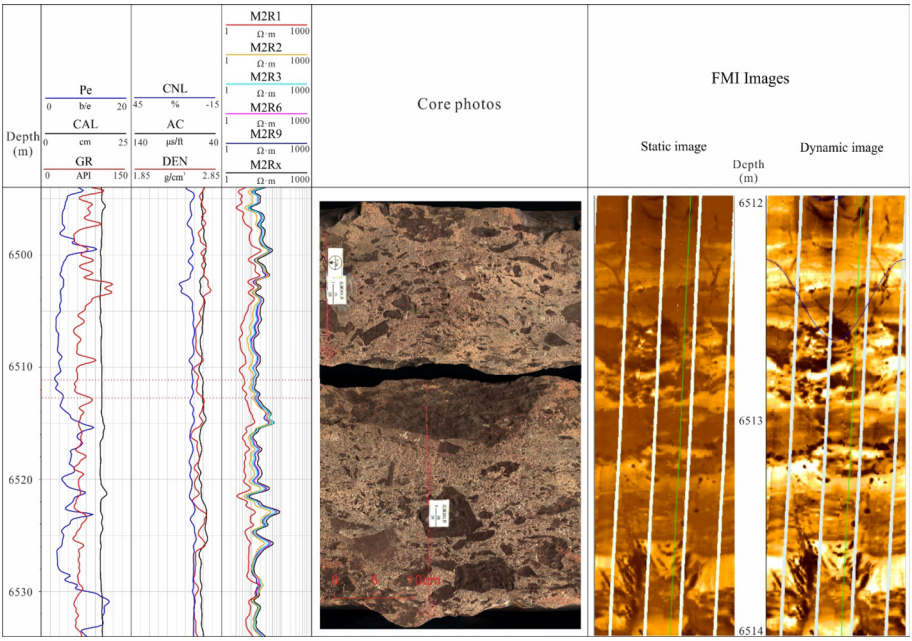

Fig. 14 Mudstone gravels show low resistivity and are recognized as dark spots on image logs (Well KS 201)

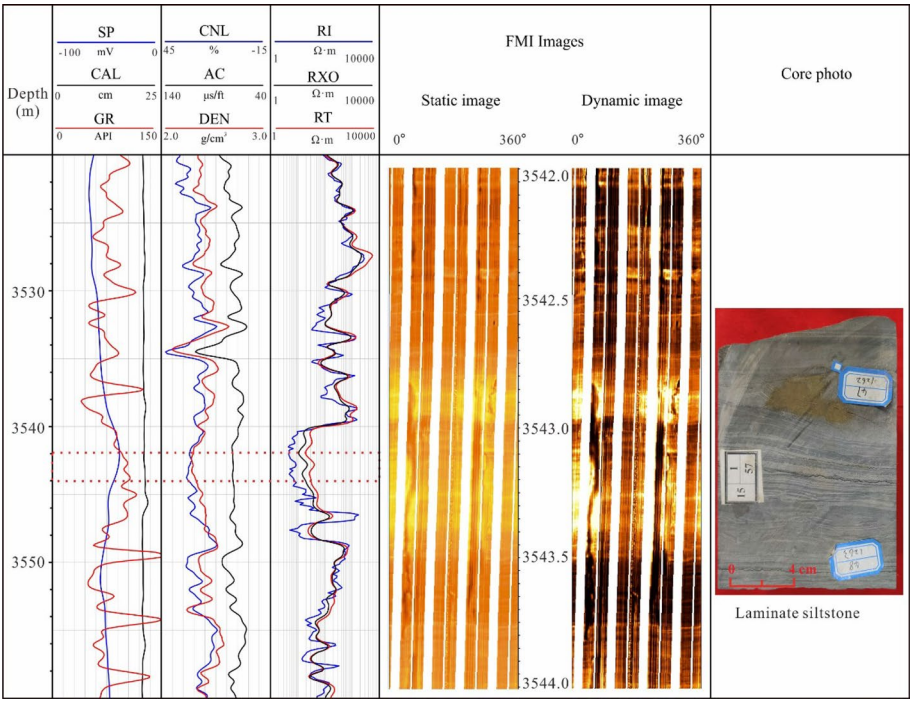

Fig. 15 High gamma sandstones due to abundance in radioactive rock fragments (Well Ji 10,025)

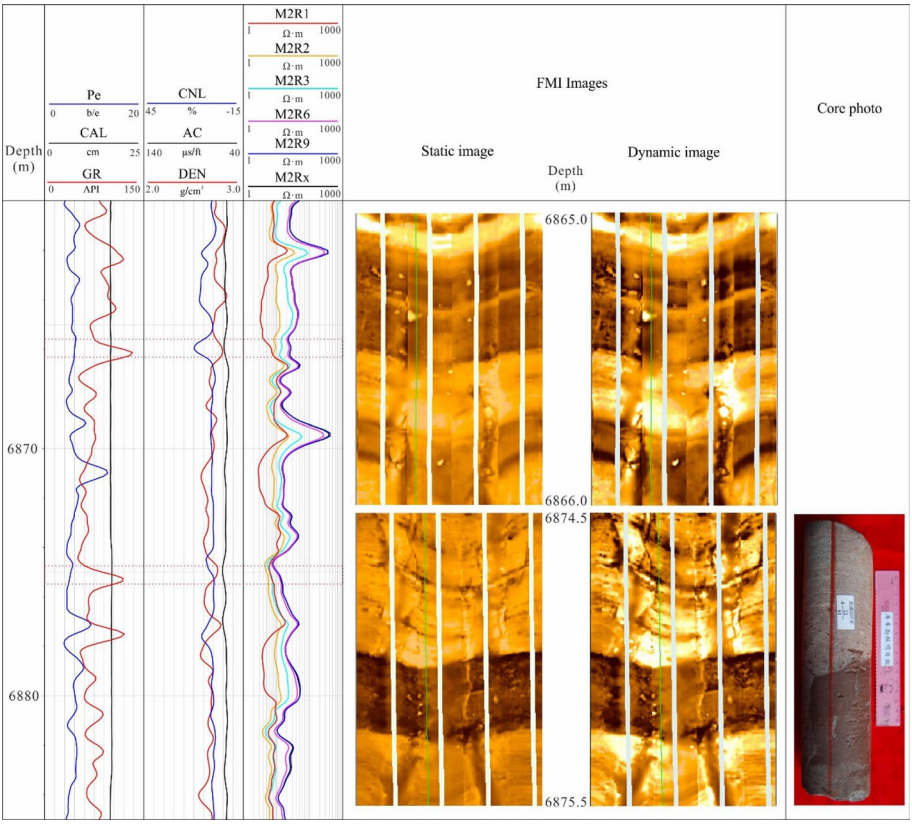

Fig. 16 High bulk density mudrocks (Well KS 207)

higher than the sandstones (Fig. 16). Besides high bulk density, some of the mudstones will show high resistivity values if they are further buried to a deeper burial depth (> 8000 m) (Fig. 17). All of the mudstone layers in Fig. 17, which are characterized by high GR values, show higher bulk density and higher resistivity readings than the surrounding sandstones (Fig. 17).

5.2 Facies Interpretation

Electrofacies is an effective way to divide the formation into depositional facies based on the varied well log responses (Ashraf et al. 2019). Gamma-ray log trends and shapes (box-shaped, funnel-shaped, bell-shaped and cylindrical-shaped) are used as an essential tool for the identification and interpretation of the subsurface depositional facies where core data are not available (Ashraf et al. 2019). In addition, electrical image logs are sensitive for the bedding planes (Fig. 18), while sonic electrical images are not, but instead can characterize the fractures even in oil based drilling muds (Fig. 19). Electrical image logs are sensitive for the presence of bedding planes, and even in oil drilling muds, the Halliburton's EI

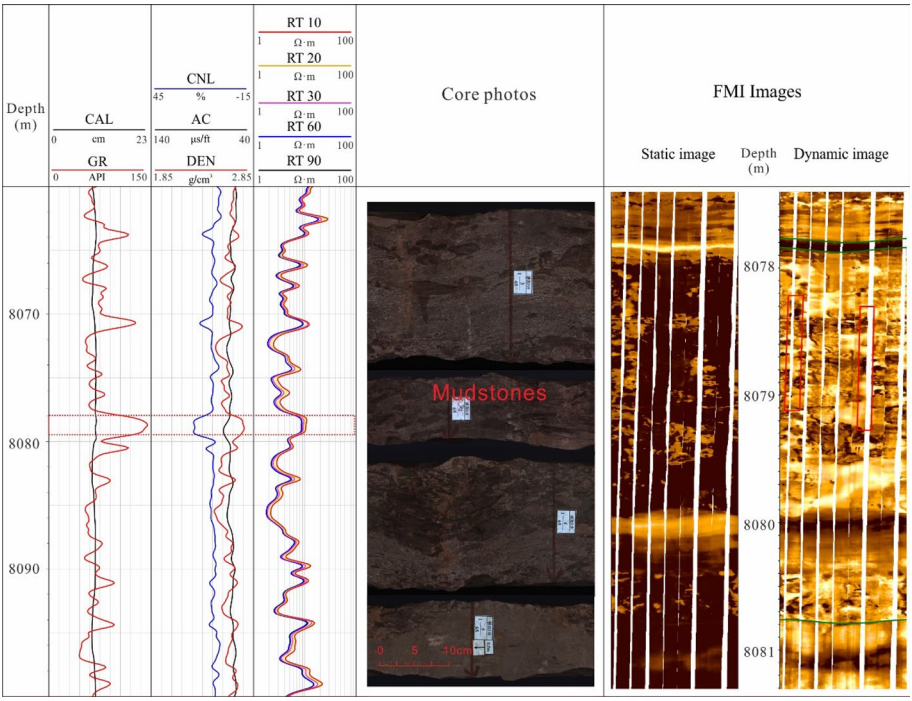

Fig. 17 High GR, high density and high resistivity mudstones (Well BZ 8)

(Earth Imager) imaging logging tool can capture the bedding planes (Fig. 18); however, they fail to recognize the open fractures. Conversely, the UXPL sonic image logs can identify the fractures, but are not sensitive for the bedding planes (Fig. 19). Therefore the typical misunderstandings will exist in the capture of sedimentary structure using image logs of poor quality.

Depositional micro-facies differ in lithology assemblage and sedimentary structures, and well logs are widely used for facies interpretation (Donselaar and Schmidt 2005; Folkestad et al. 2012; Brekke et al. 2017; He et al. 2019; Yeste et al. 2020; Feng et al. 2021; Haque et al. 2022). Therefore lithology and sedimentary structure can be characterized by well logs, and the wireline logs have the favorable ability for facies interpretation (Xu et al. 2015; Lai et al. 2018; Fan et al. 2021; Qadri et al. 2021; Leila et al. 2022). The integration of image logs and conventional logs provides a feasible method for micro-facies analysis (Fan et al. 2021). Core facies need firstly to be defined based on their lithology assemblage including composition and grain size, as well as sedimentary structure including beddings (Lai et al. 2018; He et al. 2019). Alternated siltstone and mudstone are discovered in the typical natural levee micro-facies in meandering river facies (Fig. 20). The conventional well-logs are recognized as high GR, low resistivity, and the image logs show alternated dark and bright band indicating the alternating occurrences of thin layers of siltstones and mudstones in the natural levee micro-facies (Fig. 20).

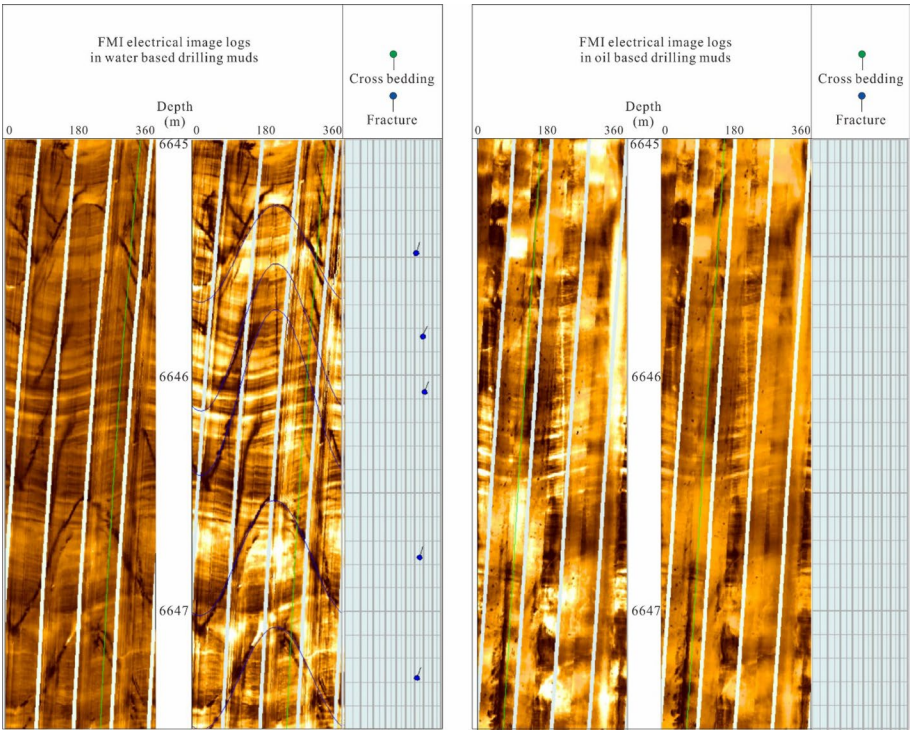

Fig. 18 Comparison of image log for bedding capture in water based and oil based drilling muds (Well KS 2–2-12)

6 Petroleum Geology

6.1 Source Rock Evaluation

Source rocks intervals containing abundant organic matters have high gamma ray (GR), high neutron porosity (CNL), high sonic transit interval time (AC), high resistivity (RT) but low bulk density (Passey et al. 1990; Iqbal et al. 2018; Stadtmuller et al. 2018; Wang et al. 2019; Shalaby et al. 2019) (Fig. 21). Besides qualitative recognition of source rocks, quantitative determination of organic matter abundance is also important. The organic richness or amounts of organics within rock can be characterized by total organic content (TOC) (Jarvie et al. 2007; Iqbal et al. 2018; Wang et al. 2019). There are a series of methods to estimate TOC content using well logs, including the ΔlogR method (Passey et al. 1990), LithoScanner method, spectral gamma ray log (*K* (%), *U* (ppm), Th (ppm)) (Sérgio et al. 2018), artificial intelligence method (artificial neural network) (Shalaby et al. 2019), etc. (Wang et al. 2019; Godfray and Seetharamaiah 2019; Lai et al. 2022c).

Therefore there are no evident misunderstandings in recognition of source rocks using well logs. However, as is known, source rocks commonly contain pyrite due to the reducing environments (Fig. 22). The occurrences of pyrites may have considerable effect of the well logs responses of source rocks. Pyrite are common heavy minerals in

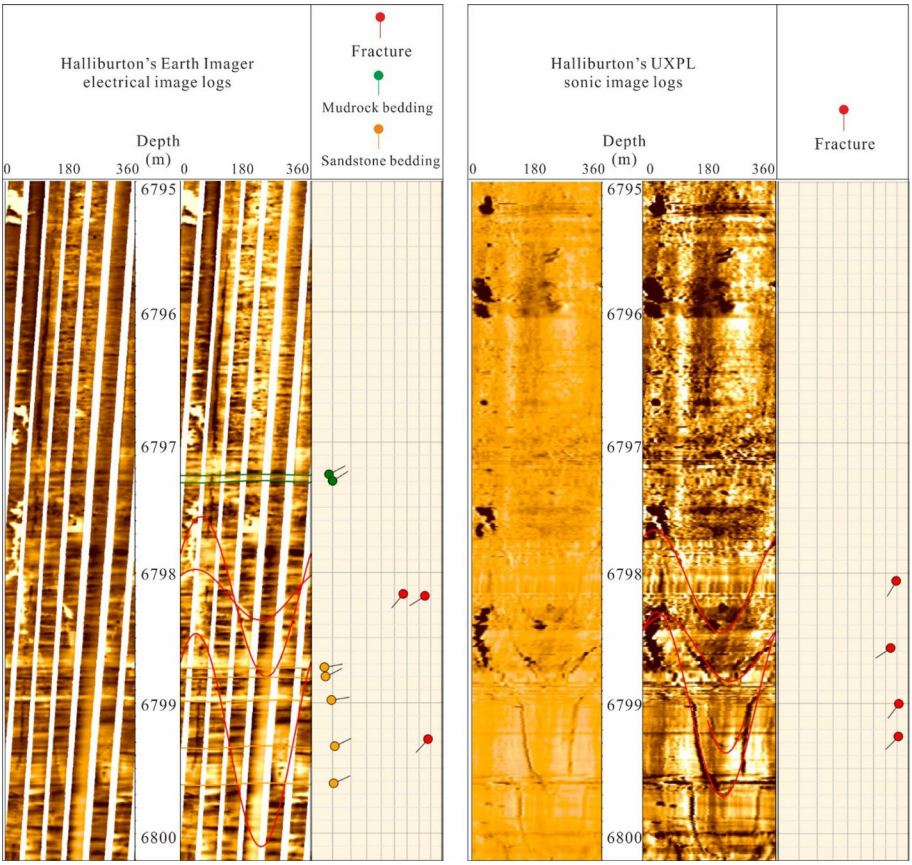

Fig. 19 Comparison of electrical and sonic image log for recognition of bedding and fractures (Well BZ 1201)

sedimentary rocks with high conductivity (Iqbal et al. 2019). Pyrites may appear as dark spot on the image logs due to their conductive properties, in addition, pyrites may result in the frequent fluctuation of resistivity logs (Fig. 21). Resistivity will be decreased in case of pyrite since pyrite is a good conductor (Wu et al. 2020). It is worth mentioning that pyrites and vugs may have similar appearances on the image logs; however, vugs are common in carbonate rocks, while in the source rocks, the vugs are rare. The most significant effect on the well logs is the nuclear magnetic resonance (NMR) log, and the NMR logs will be presented as wide T_2 (transverse relaxation time) spectrum and long tail distribution, which look like a hydrocarbon bearing reservoirs (Fig. 21).

6.2 Logging Reservoir Evaluation

Porosity and permeability are critical factors in storage and production evaluation of the energy sources (Momeni et al. 2019). Finding the hydrocarbon reserved porous reservoirs is the main proposes of geophysical well logs (Tiab and Donaldson 2004; Radwan et al. 2020). The estimation of petrophysical parameters (shale content, porosity, permeability,

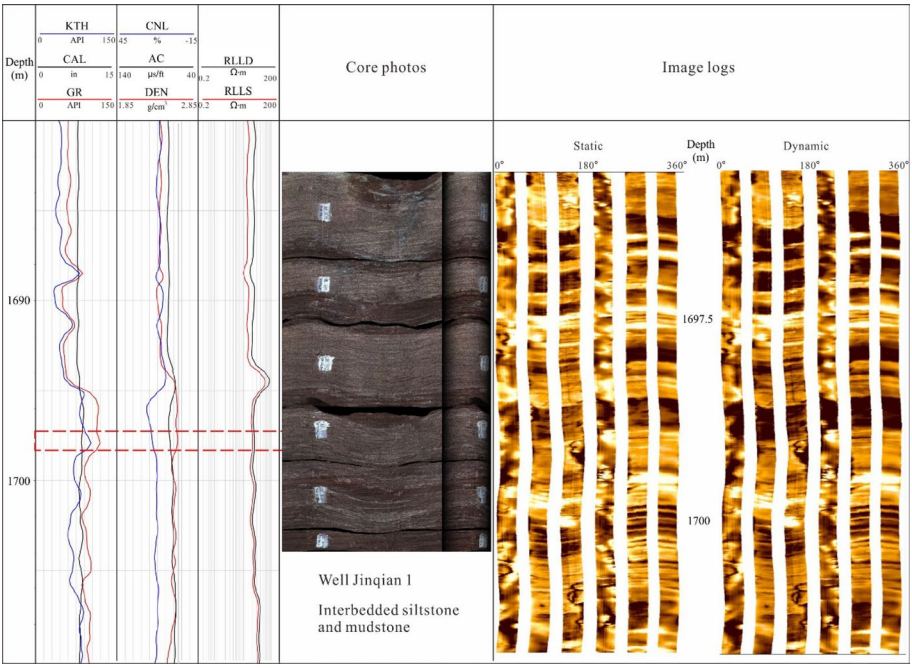

Fig. 20 Well log expressions of natural levee micro-facies in meandering river facies (Well Jinqian 1)

water saturation) plays an important role in reservoir deliverability as well as field development programs (Sen et al. 2021; Shah et al. 2021). Actually the primary purpose of the well-log analysis is to transform the raw log data into petrophysical parameters (Shah et al. 2021). Logging reservoir evaluation aims at the identification of lithology and reservoir, the calculation of reservoir parameters including porosity, permeability and hydrocarbon saturation, and then the fluid property evaluation (Ellis and Singer 2007; Iqbal et al. 2018; Shah et al. 2021). In conventional reservoirs, the logging reservoir evaluation processes are clear, and they will not be difficult challenges. However, there are evident misunderstandings in logging reservoir evaluation when encounters unconventional oil and gas resources (tight and shale oil and gas) (Lai et al. 2022c).

Self-sourced and self-retained unconventional oil and gas resources are characterized by complex lithology (various type of fine-grained sedimentary rocks), ultra-low matrix permeability and heterogeneous pore structure (Loucks et al. 2012; Li et al. 2019; Manjunath and Jha 2019; Lai et al. 2022a, b, c). Consequently, Unconventional reservoirs have remarkable differences compared with conventional reservoirs in terms of geological characteristics and well log responses (Iqbal et al. 2018; Liu et al. 2019). Horizontal well drilling and hydraulic fracturing are required for successful exploitation of unconventional hydrocarbon resources (Avanzini et al. 2016; Rybacki et al. 2016). For unconventional hydrocarbon resources, the biggest challenge in logging reservoir evaluation is how to optimize the sweet spots (favorable zones or intervals for hydrocarbon exploration) using petrophysical logs (Avanzini et al. 2016; Stadtmuller et al. 2018; Iqbal et al. 2018; Zhao et al. 2019; Qian et al. 2020; Sen et al. 2021).

Porosity reflects the capacity of fluid stored in the reservoir, and can be estimated by sonic, density and neutron logs for conventional reservoirs (Shah et al. 2021). Permeability,

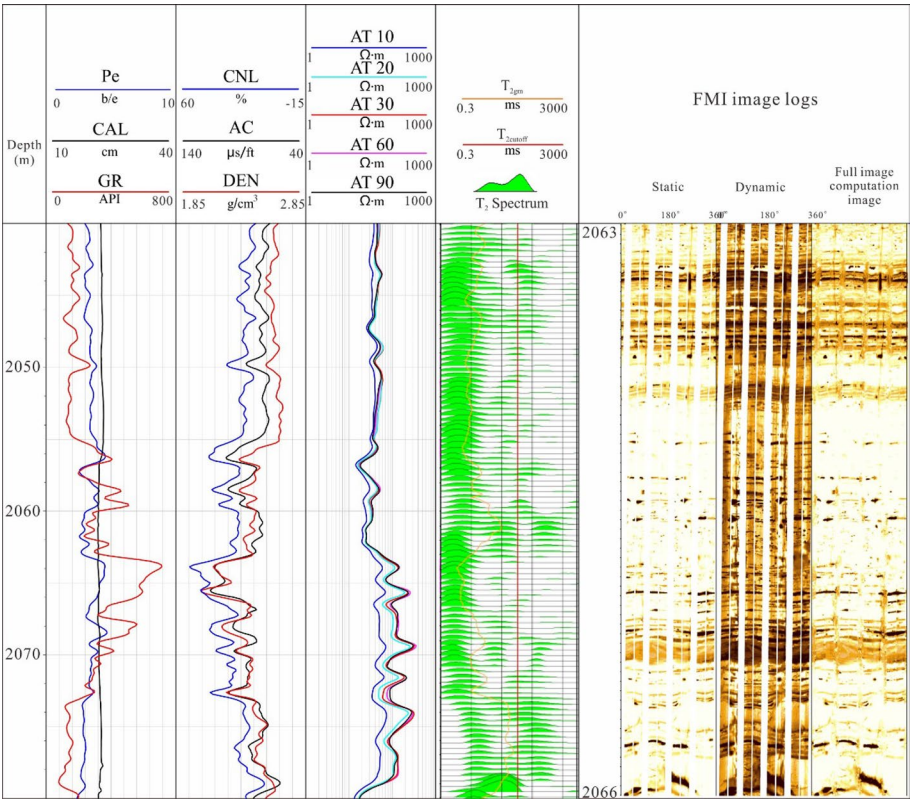

Fig. 21 Pyrite with dark spots on image logs, the presence of kerogen will affect the NMR T_2 spectrum (Well Cheng 96)

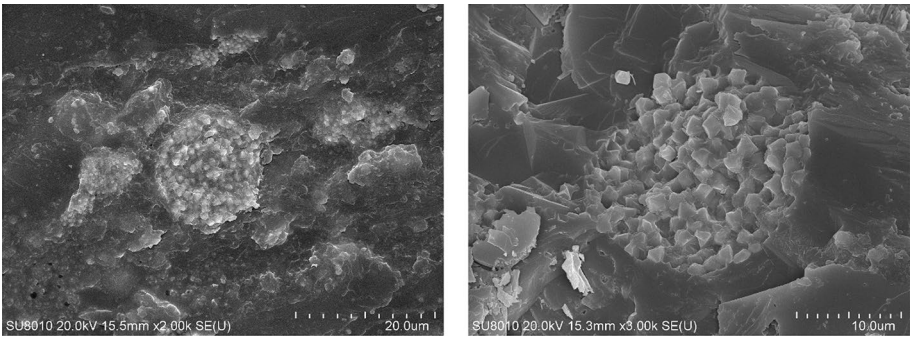

Fig. 22 SEM images showing the strawberry like pyrite in Yanchang Formation of Ordos Basin, China

which reflects flow capacity, is another fundamental and critical parameter for reservoir characterization (Zhang et al. 2021). However, conventional well log suits have no favorable ability to calculate porosity and permeability in unconventional reservoirs, especially shale oil reservoir. Water saturation are important petrophysical parameters, and neither

Archie nor Simondoux formula can be used in water saturation calculation for unconventional reservoirs (Han et al. 2021). Hydrocarbon saturation in unconventional play is difficult to be calculated due to variabilities in lithology, high clay content, low matrix porosity and presence of organic matters (Zhao et al. 2020; Kuang et al. 2020).

Advanced logging technology including NMR logs need to be integrated to calculate porosity, water saturation using iteration method, and to estimate permeability using Schlumberger Doll Research (SDR) and Coates model (Rezaee et al. 2012; Kuang et al. 2020; Liu et al. 2020; Wang et al. 2020). NMR logging is favorable to identify the fluid types in unconventional oil and gas resources since the T_1 and T_2 spectrum of oil and gas is much wider than water, and fluid property can be identified by using T_1 spectrum, T_2 spectrum as well as diffusion coefficients (Fig. 23) (Jiang et al. 2022). The oil layer and dry layer has similar well log responses on the natural gamma ray, three porosity logs, as well as resistivity logs. However, the oil layer show much wide T_2 spectrum and high T_2 amplitude than the dry layer (Fig. 23). In addition, the high-definition resistivity logs have evident separation in oil layer, while the deep resistivity (M2Rx) and shallow resistivity (M2R3) are overlapping with each other in dry layer intervals (Fig. 23). Also there are borehole collapse (enlargement in CAL) in the top intervals, resulting in the very high NMR T_2 amplitude (Fig. 23).

Fluid discrimination is challenging in reservoirs with petrophysical properties (Wang et al. 2022). Natural gas will reduce the *P*-wave velocity (*V*p) significantly, while the *S*-wave velocity (*V*s) is not sensitive for the presence of natural gas; therefore *V*p/*V*s ratio is used as a qualitative gas indicator for natural gas (Qi et al. 2017; Wang et al. 2020). Natural gas bearing layers will cause a decrease in *V*p/*V*s (Wang et al. 2020). *P*-wave impedances ($Zp = \rho \cdot Vp$) will be attenuated in case of natural gas, additionally, the Poisson's ratio (ν) will be reduced significantly due to the presence of natural gas (Russell et al. 2003; Chhun and Tsuji 2021), and the presence of natural gas reduces the *P*-wave impedances significantly. The Poisson's ratio will be reduced significantly due to the presence of natural gas (Russell et al. 2003; Qi et al. 2017; Wang et al. 2020). Therefore the array sonic logs which provide P-wave velocity, S-wave velocity, can be used to calculate the Poisson's ratio and P-wave impedances by integrating will density logs (Sohail and Hawkes 2020).

The Ordovician Majiagou dolostones in Ordos Basin are typical gas bearing reservoirs, and the typical gas layers (Layer 1, 5, 6 and 7), which are testified by the gas logging data and gas production data, have no evident reduction in Poisson's ratio and *P*-wave impedance. The *V*p/*V*s parameters are in some cases increase in these gas bearing layers (Fig. 24). The results show that the gas bearing layers in Ordovician Majiagou dolostones cannot be identified by the sonic logs.

The Ordovician Majiagou dolostones have very low porosity (< 10%) (Lai et al. 2019), and the main pore spaces are only dissolution vugs, intercrystal pores and intercrystal dissolution pores as well as microfracture, indicating a complex pore assemblage and pore structure (Fig. 25). Therefore the *V*p/*V*s method, together with Poisson's ratio and *P*-wave impedance have no ability in identifying natural gas layers in low porosity reservoirs (< 10%) (Fig. 25). The misunderstanding is that the natural gas in the very low matrix porosity has little responses on the sonic logs and related elastic parameters. Therefore in the unconventional oil and gas resources, attention needs to pay on the response contributions of the pore fluids on the wireline logs.

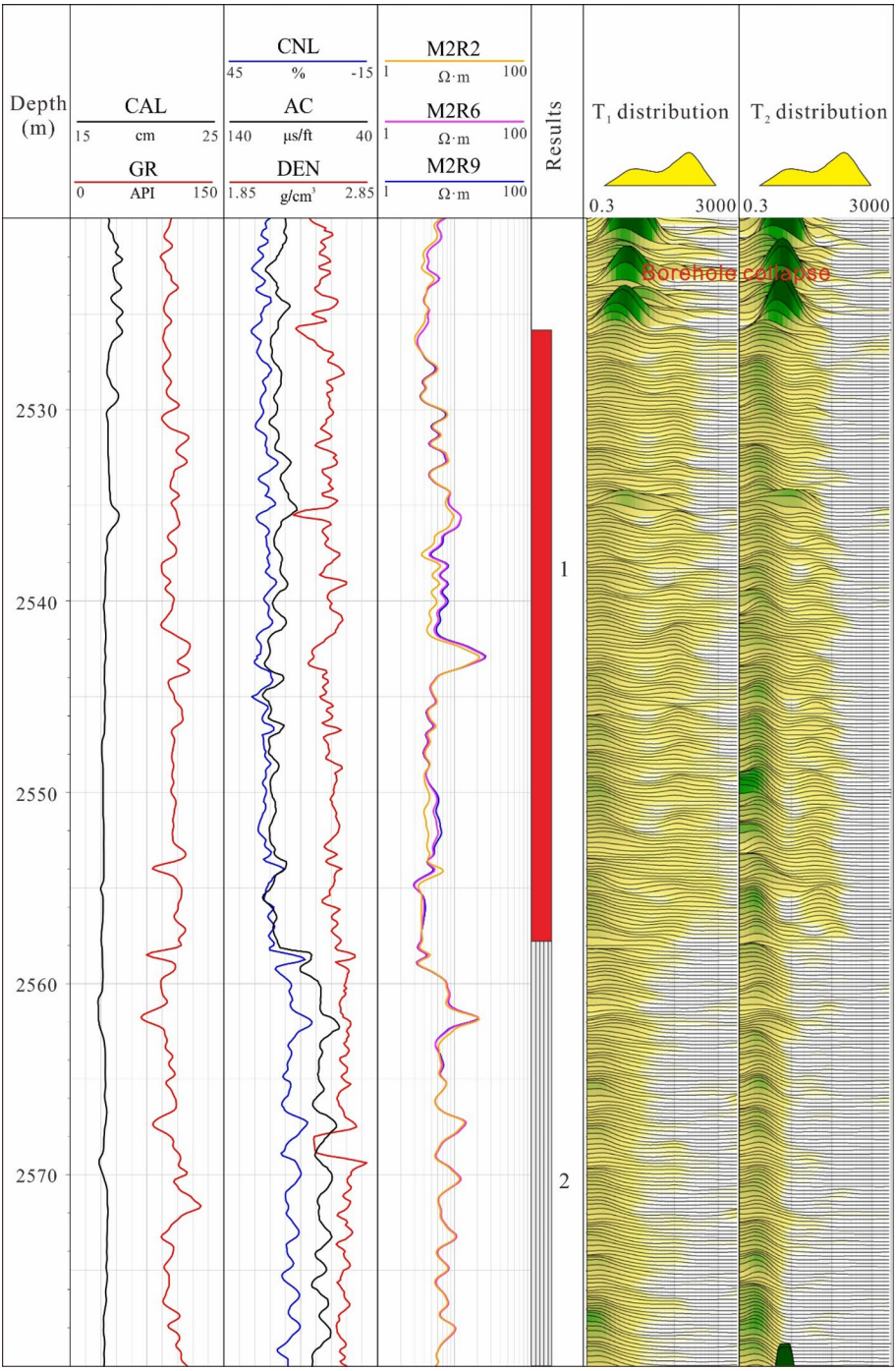

Fig. 23 Identification of oil bearing layer and dry layer using NMR log of unconventional shale reservoirs (Well GY 7)

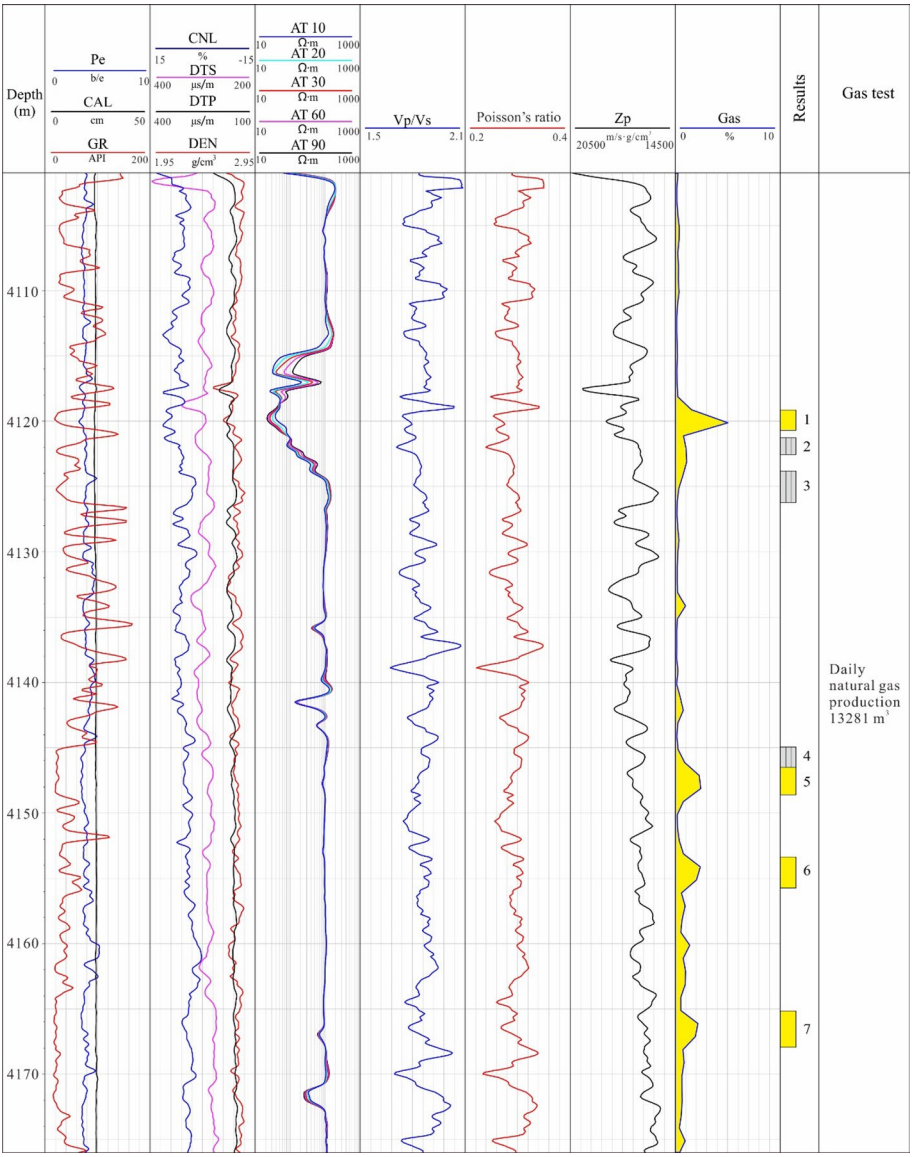

Fig. 24 Detection of gas bearing layer using Vp/Vs, wave impedance and Poisson's ratio of Ordovician Majiagou Formation dolostone in Ordos Basin (Well Su 228). Layer 1, 5, 6 and 7 are gas layers, while 2, 3 and 4 are dry layers

7 Conclusions

Types of drilling muds, borehole wall stability as well as instrument will affect the well log data acquisition and mislead the well log interpretation process. Therefore well log series should be corrected and standardized before interpretation.

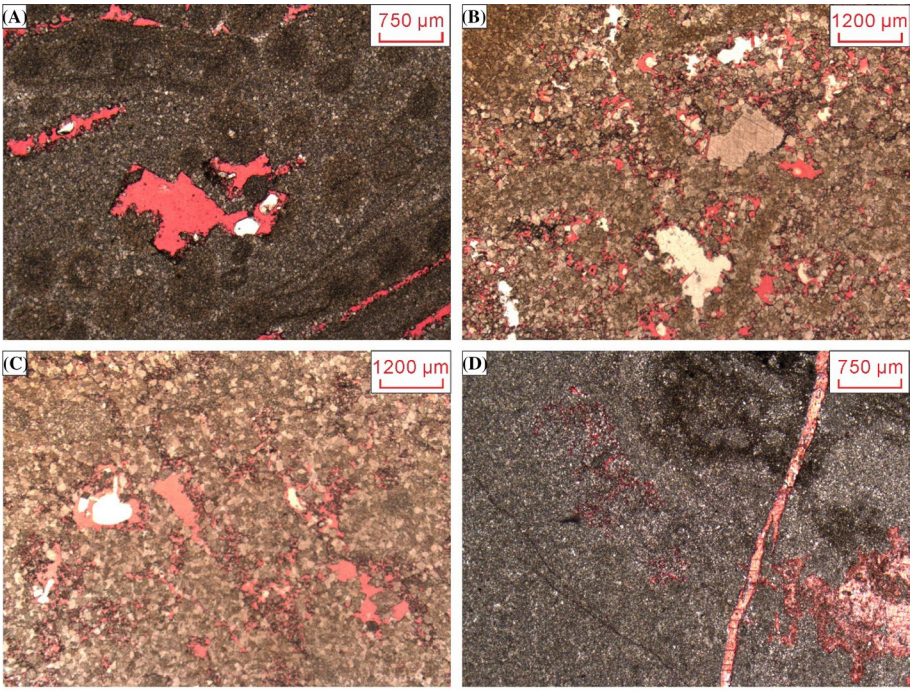

A. Dissolution vugs, Well Jin 7, 3677.10m

B. Intercrystal pores and Intercrystal dissolution pores, 3675.70m

C. Intercrystal dissolution pores, Well Jin 7, 3676.58m

D. Microfractures, Well Jin 7, 3600.28m

Fig. 25 Thin section images showing the pore spaces of Ordovician Majiagou Formation dolostones in Ordos Basin, China

Various well log suits span a wide range of vertical resolution from 5 mm to 10 m. Geological analysis data have a much higher resolution than conventional well logs, therefore attention should be paid when calibrating core data with well log data.

Well log data are used for stratum attitude determination, recognition of fault, fracture characterization, and in situ stress analysis, and unconformity evaluation in the field of structural geology. Seismic data need to be integrated to provide a correct stratum attitude parameter and for fault recognition. Fractures can be evaluated by combining conventional well logs, image log and core data.

Well logs are used for lithology recognition, and depositional facies interpretation in the field of sedimentary geology. Special lithology (high gamma sandstone, high density and high resistivity mudstone) and minerals (carbonate cemented sandstones) will mislead the well log interpretation. Electrical image logs are sensitive for the bedding planes, while sonic electrical images can instead characterize the fractures even in oil based drilling muds.

Well logs aim at source rock characterization and logging reservoir evaluation in petroleum geology. Conventional well logs fail to find the hydrocarbon and calculate reservoir parameters in low resistivity oil layers and unconventional hydrocarbon resource. Advanced well log series including NMR log and array sonic log are need in logging reservoir evaluation. Petrophysical well logs are a comprehensive reflection of lithology, porosity, fluid type and borehole environments, and petrophysicists should analyze the controlling factors which determine the high fluctuation of well logs.

Acknowledgments This work is financially supported by National Natural Science Foundation of China (Grant No. 42002133, 41872133), strategic cooperation project of PetroChina and CUPB (China University of Petroleum, Beijing) (ZLZX2020-01) and Science Foundation of CUPB (No. 2462021YXZZ003). The authors would like to express their sincere thanks to the PetroChina Xinjiang, Southwest, Changqing, Tarim and Jidong Oilfield for their assistance in providing the information, and for their technical input to this work.

References

Aghli G, Soleimani B, Moussavi-Harami R, Mohammadian R (2016) Fractured zones detection using conventional petrophysical logs by differentiation method and its correlation with image logs. J Petrol Sci Eng 142:152–162

Aghli G, Moussavi-Harami R, Mortazavi S, Mohammadian R (2019) Evaluation of new method for estimation of fracture parameters using conventional petrophysical logs and ANFIS in the carbonate heterogeneous reservoirs. J Petrol Sci Eng 172:1092–1102

Aghli G, Moussavi-Harami R, Mohammadian R (2020) Reservoir heterogeneity and fracture parameter determination using electrical image logs and petrophysical data (a case study, carbonate Asmari Formation, Zagros Basin, SW Iran). Petrol Sci 17:51–69

Al-Mudhafar WJ (2020) Integrating machine learning and data analytics for geostatistical characterization of clastic reservoirs. J Petrol Sci Eng 195:107837

Ameen MS (2014) Fracture and in-situ stress patterns and impact on performance in the khuff structural prospects, eastern offshore Saudi Arabia. Mar Pet Geol 50(50):166–184

Ameen MS (2016) Fracture modes in the Silurian Qusaiba shale play, northern Saudi Arabia and their geomechanical implications. Mar Pet Geol 78:312–355

Ameen MS, MacPherson K, Al-Marhoon MI, Rahim Z (2012) Diverse fracture properties and their impact on performance in conventional and tight-gas reservoirs, Saudi Arabia: the Unayzah South Haradh Case Study. AAPG Bull 96(3):459–492

Ashraf U, Zhu P, Yasin Q, Anees A, Imraz M, Mangi HN, Shakeel S (2019) Classification of reservoir facies using well log and 3D seismic attributes for prospect evaluation and field development: a case study of Sawan gas field, Pakistan. J Petrol Sci Eng 175:338–351

Avanzini A, Balossino P, Brignoli M, Spelta E, Tarchiani C (2016) Lithologic and geomechanical facies classification for sweet spot identification in gas shale reservoir. Interpretation 4(3):SL21–SL31

Brekke H, MacEachern JA, Roenitz T, Dashtgard SE (2017) The use of microresistivity image logs for facies interpretations: an example in point-bar deposits of the McMurray Formation, Alberta, Canada. AAPG Bull 101(5):655–682

Chhun C, Tsuji T (2021) Pore pressure and gas saturation distribution in the forearc basin of the Nankai subduction zone inferred from high-resolution Vp and Vs. J Petrol Sci Eng 205:108911

Collett TS, Lewis RE, Winters WJ, Lee MW, Rose KK, Boswell RM (2011) Downhole well log and core montages from the Mount Elbert gas hydrate stratigraphic test well, Alaska north slope. Mar Pet Geol 28:561–577

Donselaar ME, Schmidt JM (2005) Integration of outcrop and borehole image logs for high-resolution facies interpretation: example from a fluvial fan in the Ebro Basin, Spain. Sedimentology 52:1021–1042

Ellis DV, Singer JM (2007) Well logging for Earth Scientists, 2nd edn. Springer, Dordrecht

Fan H, Shi J, Fan T, Gao Z, Gu Y, Gao Z, Zhang T, Li Y, Li B (2021) Sedimentary microfacies analysis of carbonate formation based on FMI and conventional logs: a case study from the Ordovician in the Tahe Oilfield, Tarim Basin, China. J Petrol Sci Eng 203:108603

Feng Q, Xiao Y, Hou X, Chen H, Wang Z, Feng Z, Tian H, Jiang H (2021) Logging identification method of depositional facies in Sinian Dengying formation of the Sichuan Basin. Pet Sci 18:1086–1096

Folkestad A, Veselovsky Z, Roberts P (2012) Utilising borehole image logs to interpret delta to estuarine system: A case study of the subsurface Lower Jurassic Cook formation in the Norwegian northern North Sea. Mar Pet Geol 29:255–275

Godfray G, Seetharamaiah J (2019) Geochemical and well logs evaluation of the Triassic source rocks of the Mandawa basin, SE Tanzania: implication on richness and hydrocarbon generation potential. J Afr Earth Sci 153:9–16

Han TC, Yan H, Fu LY (2021) A quantitative interpretation of the saturation exponent in Archie's equations. Pet Sci 18:444–449

Haque AKME, Qadri SMT, Bhuiyan MAH, Navid M, Nabawy BS, Hakimi MH, Abd-El-Aal AK (2022) Integrated wireline log and seismic attribute analysis for the reservoir evaluation: a case study of the Mount Messenger Formation in Kaimiro Field, Taranaki Basin, New Zealand. J Nat Gas Sci Eng 99:104452

He J, Croix ADL, Wang J, Ding W, Underschultz JR (2019) Using neural networks and the Markov Chain approach for facies analysis and prediction from well logs in the Precipice Sandstone and Evergreen Formation, Surat Basin, Australia. Mar Pet Geol 101:410–427

Hsieh BZ, Lewis C, Lin Z (2005) Lithology identification of aquifers from geophysical well logs and fuzzy logic analysis: Shui-Lin Area, Taiwan. Comput Geosci 31:263–275

Iqbal O, Ahmad M, Kadir A (2018) Effective evaluation of shale gas reservoirs by means of an integrated approach to petrophysics and geomechanics for the optimization of hydraulic fracturing: a case study of the Permian Roseneath and Murteree Shale Gas reservoirs, Cooper Basin, Australia. J Nat Gas Sci Eng 58:34–58

Iqbal MA, Salim AMA, Baioumy H, Gaafar GR, Wahi A (2019) Identification and characterization of low resistivity low contrast zones in a clastic outcrop from Sarawak, Malaysia. J Appl Geophys 160:207–217

Jafari A, Kadkhodaie-IIkhchi A, Sharghi Y, Ghanavati K (2012) Fracture density estimation from petrophysical log data using the adaptive neuro-fuzzy inference system. J Geophys Eng 9:105–114

Jarvie DM, Hill RJ, Ruble TE (2007) Unconventional shale-gas systems: the Mississippian Barnett Shale of north-central Texas as one model for thermogenic shale-gas assessment. AAPG Bull 91:475–499

Jiang Z, Liu Z, Zhao P, Chen Z, Mao Z (2022) Evaluation of tight waterflooding reservoirs with complex wettability by NMR data: a case study from Chang 6 and 8 members, Ordos Basin, NW China. J Petrol Sci Eng 213:110436

Josh M, Esteban L, Delle PC, Sarout J, Dewhurst DN, Clennell MB (2012) Laboratory characterisation of shale properties. J Petrol Sci Eng 88–89:107–124

Keeton G, Pranter M, Cole RD, Gustason ER (2015) Stratigraphic architecture of fluvial deposits from borehole images, spectral-gamma-ray response, and outcrop analogs, Piceance Basin, Colorado. AAPG Bull 99(10):1929–1956

Khair HA, Cooke D, Hand M (2015) Paleo stress contribution to fault and natural fracture distribution in the Cooper Basin. J Struct Geol 79:31–41

Khoshbakht F, Azizzadeh M, Memarian H, Nourozi GH, Moallemi SA (2012) Comparison of electrical image log with core in a fractured carbonate reservoir. J Petrol Sci Eng 86–87:289–296

Kuang L, Wang Z, Feng C, Zhao P, Mao R, Yu J (2020) Predicting oil saturation of shale-oil reservoirs using nuclear magnetic resonance logs. Interpretation 8(3):SL35–SL43

Lai J, Wang G, Huang L, Li W, Ran Y, Wang D, Zhou Z, Chen J (2015) Brittleness index estimation in a tight shaly sandstone reservoir using well logs. J Nat Gas Sci Eng 27:1536–1545

Lai J, Wang G, Chai Y, Ran Y (2016) Prediction of diagenetic facies using well logs: evidences from Upper Triassic Yanchang Formation Chang 8 sandstones in Jiyuan Region, Ordos Basin, China. Oil Gas Sci Technol 71:34

Lai J, Wang G, Fan Z, Wang Z, Chen J, Zhou Z, Wang S, Xiao C (2017) Fracture detection in oil-based drilling mud using a combination of borehole image and sonic logs. Mar Pet Geol 84:195–214

Lai J, Wang G, Wang S, Cao J, Li M, Pang X, Han C, Fan X, Yang L, He Z, Qin Z (2018) A review on the applications of image logs in structural analysis and sedimentary characterization. Mar Pet Geol 95:139–166

Lai J, Pang X, Xiao Q, Shi Y, Zhang H, Zhao T, Chen J, Wang G, Qin Z (2019) Prediction of reservoir quality in carbonates via porosity spectrum from image logs. J Petrol Sci Eng 173:197–208

Lai J, Wang S, Zhang C, Wang G, Song Q, Chen X, Yang K, Yuan C (2020) Spectrum of pore types and networks in the deep Cambrian to Lower Ordovician dolostones in Tarim Basin, China. Mar Petrol Geol 112:104081

Lai J, Liu S, Xin Y, Wang S, Xiao C, Song Q, Chen X, Wang G, Qin Z, Ding X (2021) Geological-petrophysical insights in the deep Cambrian dolostone reservoirs in Tarim Basin, China. AAPG Bull 105(11):2263–2296

Lai J, Pang X, Zhao X, Zhao Y, Wang G, Huang Y, Li H, Li Y (2022a) Typical misunderstandings and scientific ideas in well logging geology research. Nat Gas Ind 42(7):31–44 ((**in Chinese**))

Lai J, Liu B, Li H, Pang X, Liu S, Bao M, Wang G (2022b) Bedding parallel fractures in fine-grained sedimentary rocks: recognition, formation mechanisms, and prediction using well log. Pet Sci 19(2):554–569

Lai J, Wang G, Fan Q, Pang X, Li H, Zhao F, Li Y, Zhao X, Zhao Y, Huang Y, Bao M, Qin Z, Wang Q (2022c) Geophysical well log evaluation in the era of unconventional hydrocarbon resources: a review on current status and prospects. Surv Geophys 43:913–957

Leila M, Yasser A, Bastawesy ME, Mahmoudi AE (2022) Seismic stratigraphy, sedimentary facies analysis and reservoir characteristics of the Middle Jurassic syn-rift sediments in Salam Oil Field, north Western Desert, Egypt. Mar Petrol Geol 136:105466

Li R, Li Y (2011) The geologic features of mineralization at the Dongsheng uranium deposit in the northern Ordos Basin (Central China). Russ Geol Geophys 52(6):593–602

Li M, Chen Z, Ma X, Cao T, Qian M, Jiang Q, Tao G, Li Z, Song G (2019) Shale oil resource potential and oil mobility characteristics of the Eocene-Oligocene Shahejie Formation, Jiyang Super-Depression, Bohai Bay Basin of China. Int J Coal Geol 204:130–143

Liu Q, Chen M, Liu W, Li J, Han P, Guo Y (2009) Origin of natural gas from the Ordovician paleo-weathering crust and gas-filling model in Jingbian gas field, Ordos basin, china. J Asian Earth Sci 35(1):74–88

Liu B, Wang H, Fu X, Bai Y, Bai L, Jia M, He B (2019) Lithofacies and depositional setting of a highly prospective lacustrine shale oil succession from the Upper Cretaceous Qingshankou Formation in the Gulong sag, northern Songliao Basin, northeast China. AAPG Bull 103(2):405–432

Liu X, Lai J, Fan X, Shu H, Wang G, Ma X, Liu M, Guan M, Luo Y (2020) Insights in the pore structure, fluid mobility and oiliness in oil shales of Paleogene Funing Formation in Subei Basin, China. Mar Petrol Geol 114:104228

Loucks RG, Reed RM, Ruppel SC, Hammes U (2012) Spectrum of pore types and networks in mudrocks and a descriptive classification for matrix-related mudrock pores. AAPG Bull 96:1071–1098

Lyu W, Zeng L, Liu Z, Liu G, Zu K (2016) Fracture responses of conventional logs in tight-oil sandstones: a case study of the Upper Triassic Yanchang Formation in southwest Ordos Basin, China. AAPG Bull 100(9):1399–1417

Manjunath GL, Jha B (2019) Geomechanical characterization of gondwana shale across nano-micro-meso scales. Int J Rock Mech Min Sci 119:35–45

Masoudi P, Aïfa T, Memarian H, Tokhmechi B (2017) Uncertainty assessment of volumes of investigation to enhance the vertical resolution of well-logs. J Petrol Sci Eng 154:252–276

Mollajan A, Memarian H (2016) Rock physics-based carbonate pore type identification using Parzen classifier. J Petrol Sci Eng 145:205–212

Momeni A, Rostamia S, Hashemi S, Mosalman-Nejad H, Ahmadi A (2019) Fracture and fluid flow paths analysis of an offshore carbonate reservoir using oil-based mud images and petrophysical logs. Mar Pet Geol 109:349–360

Moussavi-Harami R, Mohammadian R (2016) Fractured zones detection using conventional petrophysical logs by differentiation method and its correlation with image logs. J Petrol Sci Eng 142:152–162

Nelson R (2001) Geologic analysis of naturally fractured reservoirs. Gulf Professional Publishing, pp 96–104

Ngia NR, Hu M, Gao D (2019) Tectonic and geothermal controls on dolomitization and dolomitizing fluid flows in the Cambrian-Lower Ordovician carbonate successions in the western and central Tarim Basin, NW China. J Asian Earth Sci 172:359–382

Nian T, Wang G, Tan C, Fei L, He W, Wang S (2021) Hydraulic apertures of barren fractures in tight-gas sandstones at depth: Image-core calibration in the lower cretaceous Bashijiqike Formation, Tarim Basin. J Petrol Sci Eng 196:108016

Okoli AE, Agbasi OE, Lashin AA, Sen S (2021) Static reservoir modeling of the Eocene clastic reservoirs in the Q-Field, Niger Delta, Nigeria. Nat Resour Res 30(2):1411–1425

Pan X, Lu C, Zhang G, Wang P, Liu J (2022) Seismic characterization of naturally fractured reservoirs with monoclinic symmetry induced by horizontal and tilted fractures from amplitude variation with offset and azimuth. Surv Geophys 43:815–851

Pang X, Wang G, Kuang L, Li H, Zhao Y, Li D, Zhao X, Wu S, Feng Z, Lai J (2022) Insights into the pore structure and oil mobility in fine-grained sedimentary rocks: the Lucaogou Formation in Jimusar Sag, Junggar Basin, China. Mar Petrol Geol 137:105492

Passey Q, Creaney S, Kulla J, Moretti F, Stroud J (1990) A practical model for organic richness from porosity and resistivity logs. AAPG Bull 74:1777–1794
Prioul R, Donald A, Koepsell R, Marzouki ZE, Bratton T (2007) Forward modeling of fracture-induced sonic anisotropy using a combination of borehole image and sonic logs. Geophysics 72(4):135–147
Qadri SMT, Islam MA, Shalaby MR (2019) Application of well log analysis to estimate the petrophysical parameters and evaluate the reservoir quality of the Lower Goru Formation, Lower Indus Basin, Pakistan. Geomech Geophys Geo-Energy Geo-Resour 5:271–288
Qadri SMT, Islam MA, Shalaby M-A, A.K.A, (2021) Reservoir quality evaluation of the Farewell sandstone by integrating sedimentological and well log analysis in the Kupe South Field, Taranaki Basin-New Zealand. J Petrol Explor Prod 11:11–31
Qadri SMT, Ahmed W, Haque AKME, Radwan AE, Hakimi MH, Abdel Aal AK (2022) Murree clay problems and water-based drilling mud optimization: a case study from the Kohat Basin in Northwestern Pakistan. Energies 15:3424
Qi QM, Müller TM, Pervukhina M (2017) Sonic QP/QS ratio as diagnostic tool for shale gas saturation. Geophysics 82(3):MR97–MR103
Qian K, Liu T, Liu J, Liu X, He Z, Jiang D (2020) Construction of a novel brittleness index equation and analysis of anisotropic brittleness characteristics for unconventional shale formations. Pet Sci 17:70–85
Qiu JT, Mu H, Yu X, Rui X, Yang Y, Qiu L (2022) Identifying the principal factors controlling uranium enrichment: Semi-quantitative mineralogy and geochemistry of the sandstone-type Qianjiadian uranium deposit, northeast China. Ore Geol Rev 144:104807
Radwan AE, Abudeif AM, Attia MM (2020) Investigative petrophysical fingerprint technique using conventional and synthetic logs in siliciclastic reservoirs: a case study, Gulf of Suez basin, Egypt. J Afr Earth Sci 167:103868
Rezaee R, Saeedi A, Clennell B (2012) Tight gas sands permeability estimation from mercury injection capillary pressure and nuclear magnetic resonance data. J Petrol Sci Eng 88–89:92–99
Russell BH, Hedlin K, Hilterman FJ, Lines LR (2003) Fluid-property discrimination with AVO: a Biot-Gassmann perspective. Geophysics 68(1):29–39
Rybacki E, Meier T, Dresen G (2016) What controls the mechanical properties of shale rocks?—Part II: Brittleness. J Petrol Sci Eng 144:39–58
Sarhan MA (2019) Seismic delineation and well logging evaluation for albian Kharita Formation, South West Qarun (SWQ) field, Gindi Basin, Egypt. J Afr Earth Sci 158:103544
Sen S, Abioui M, Ganguli SS, Elsheikh A, Debnath A, Benssaou M, Abdelhady AA (2021) Petrophysical heterogeneity of the early Cretaceous Alamein dolomite reservoir from North Razzak oil field, Egypt integrating well logs, core measurements, and machine learning approach. Fuel 306:121698
Sérgio SLR, Duarte LV, Pereira AJSC, Silva RL (2018) Field gamma-ray patterns and stratigraphic reinterpretation of offshore well-log data from lower Jurassic organic-rich units of the Lusitanian Basin (Portugal). Mar Pet Geol 98:860–872
Shah MS, Khan MHR, Rahman A, Islam MR, Ahmed SI, Molla MI, Butt S (2021) Petrophysical evaluation of well log data for reservoir characterization in Titas gas field, Bangladesh: a case study. J Nat Gas Sci Eng 95:104129
Shalaby MR, Jumat N, Lai D, Malik O (2019) Integrated TOC prediction and source rock characterization using machine learning, well logs and geochemical analysis: Case study from the Jurassic source rocks in Shams Field, NW Desert, Egypt. J Petrol Sci Eng 176:369–380
Shan L, Liu Y, Tang M, Yang M, Bai X (2021) CNN-BiLSTM hybrid neural networks with attention mechanism for well log prediction. J Petrol Sci Eng 205:108838
Sohail GM, Hawkes CD (2020) An evaluation of empirical and rock physics models to estimate shear wave velocity in a potential shale gas reservoir using wireline logs. J Petrol Sci Eng 185:106666
Stadtmuller M, Lis-Sledziona A, Słota-Valim M (2018) Petrophysical and geomechanical analysis of the lower Paleozoic shale formation, North Poland. Interpretation 6(3):91–106
Tiab D, Donaldson EC (2004) Petrophysics: theory and practice of measuring reservoir rock and fluid transport properties, 2nd edn. Elsevier
Tian F, Luo X, Zhang W (2019) Integrated geological-geophysical characterizations of deeply buried fractured-vuggy carbonate reservoirs in Ordovician strata, Tarim Basin. Mar Pet Geol 99:292–309
Wang B, Al-Aasm IS (2002) Karst-controlled diagenesis and reservoir development: example from the Ordovician main-reservoir carbonate rocks on the eastern margin of the Ordos basin, China. AAPG Bull 86(9):1639–1658
Wang H, Wu W, Chen T, Dong X, Wang G (2019) An improved neural network for TOC, S1 and S2 estimation based on conventional well logs. J Petrol Sci Eng 176:664–678
Wang G, Lai J, Liu B, Fan Z, Liu S, Shi Y, Zhang H, Chen J (2020) Fluid property discrimination in dolostone reservoirs using well logs. Acta Geologica Sinica (english Edition) 94(3):831–846

Wang P, Cui Y, Liu J (2022) Fluid discrimination based on inclusion-based method for tight sandstone reservoirs. Surv Geophys 43:1469–1496

Wu Y, Lin C, Yan W, Liu Q, Zhao P, Ren L (2020) Pore-scale simulations of electrical and elastic properties of shale samples based on multicomponent and multiscale digital rocks. Mar Pet Geol 117:104369

Xu C, Cronin TP, McGinness TE, Steer B (2009) Middle Atokan sediment gravity flows in the Red Oak field, Arkoma Basin, Oklahoma: a sedimentary analysis using electrical borehole images and wireline logs. AAPG Bull 93(1):1–29

Xu C, Gehenn JM, Zhao D, Xie G, Teng MK (2015) The fluvial and lacustrine sedimentary systems and stratigraphic correlation in the Upper Triassic Xujiahe Formation in Sichuan Basin, China. AAPG Bull 99(11):2023–2041

Yang Y, Li W, Ma L (2005) Tectonic and stratigraphic controls of hydrocarbon systems in the Ordos basin: a multicycle cratonic basin in central China. AAPG Bull 89(2):255–269

Yeste LM, Varela AN, Viseras C, Mcdougall ND, Garcia-Garcia F (2020) Reservoir architecture and heterogeneity distribution in floodplain sandstones: key features in outcrop, core and wireline logs. Sedimentology 67:3355–3388

Zaree V, Riahi MA, Khoshbakht F, Hemmati HR (2016) Estimating fracture intensity in hydrocarbon reservoir: an approach using DSI data analysis. Carbonates Evaporites 31:101–107

Zazoun RS (2013) Fracture density estimation from core and conventional well logs data using artificial neural networks: the Cambro-Ordovician reservoir of Mesdar oil field, Algeria. J Afr Earth Sc 83:55–73

Zeng L, Li X (2009) Fractures in sandstone reservoirs with ultra-low permeability: a case study of the Upper Triassic Yanchang formation in the Ordos Basin, China. AAPG Bull 93(4):461–477

Zhang Z, Zhang H, Li J, Cai Z (2021) Permeability and porosity prediction using logging data in a heterogeneous dolomite reservoir: an integrated approach. J Nat Gas Sci Eng 86:103743

Zhao X, Zhou L, Pu X, Han W, Jin F, Xiao D, Shi Z, Deng Y, Zhang W, Jiang W (2019) Exploration breakthroughs and geological characteristics of continental shale oil: a case study of the Kongdian Formation in the Cangdong Sag, China. Mar Pet Geol 102:544–556

Zhao P, Fu J, Shi Y, Li G, Ostadhassan M, Luo M, Mao Z (2020) Hydrocarbon saturation in shale oil reservoirs by inversion of dielectric dispersion logs. Fuel 266:116934